Quark helicity PDFs of proton from lattice QCD

Hai-Tao Shu

for the ANL/BNL collaboration

BNL —> CCNU

The 4th EIC-Asia Workshop

Jul 1-5, 2024, Shanghai, China

What is quark helicity PDF?

The probability of finding a parton (constituent quark) with momentum fraction *x* in a longitudinally polarized fast-moving proton

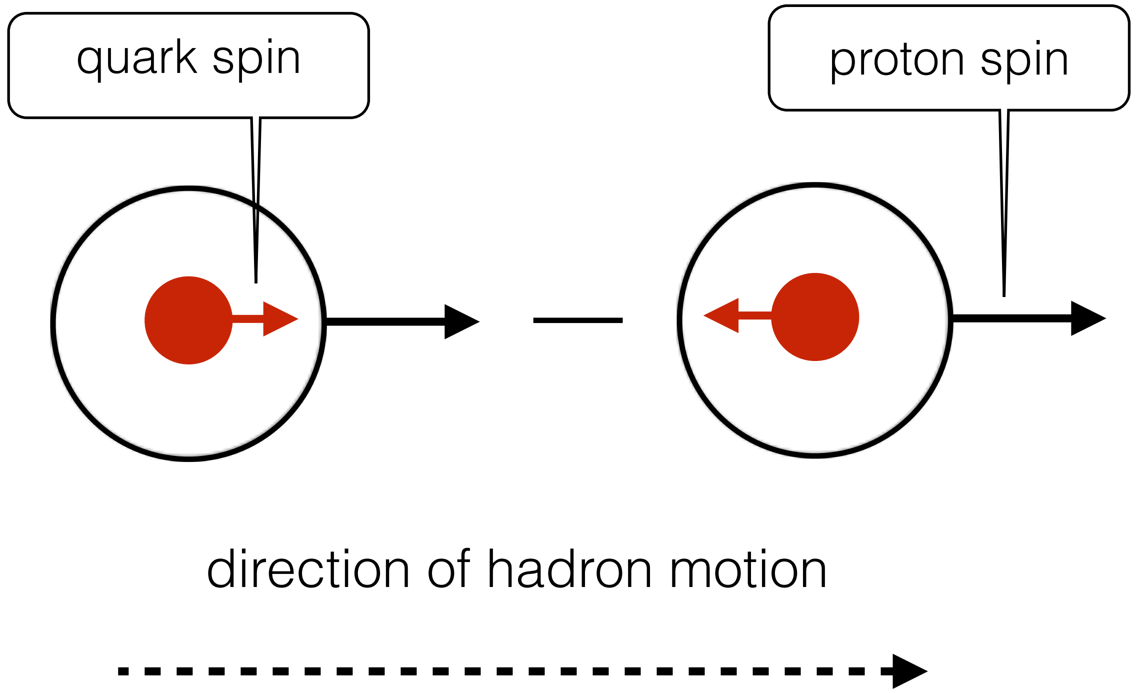

Why is it important?

Jaffe-Manohar/Ji spin sum rule:

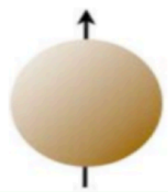

$$\frac{1}{2} = \frac{1}{2}\Delta\Sigma + \Delta G + (L_q + L_g) = \sum \langle P, S | \hat{J}^z_f(\mu) | P, S \rangle$$

Proton Spin

[Jaffe and Manohar, NPB 337, 509 (1990)]
[Ji, PRL. 78, 610 (1997)]

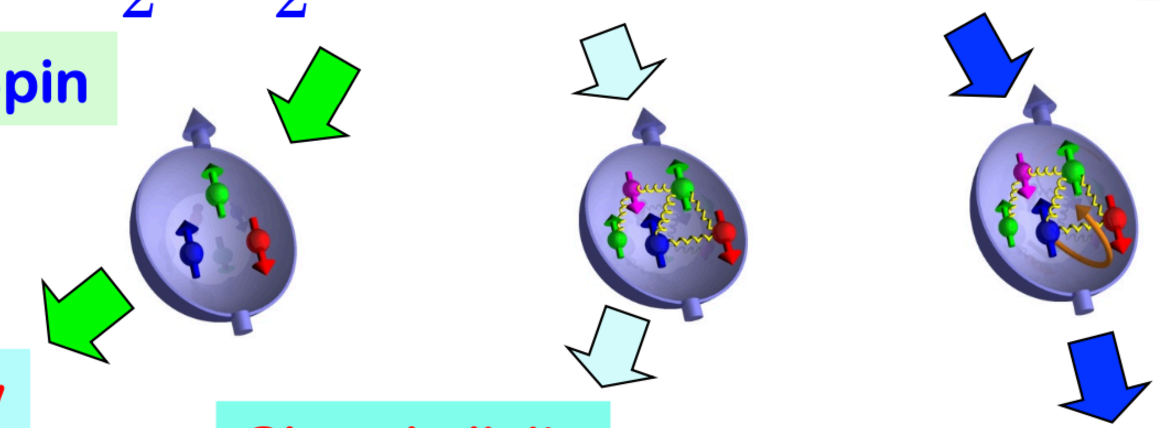

Quark helicity
Best known

$$\frac{1}{2}\int dx \left(\Delta u + \Delta\bar{u} + \Delta d + \Delta\bar{d} + \Delta s + \Delta\bar{s}\right)$$

$$\sim 30\%$$

Spin "puzzle"

Gluon helicity
Start to know

$$\Delta G = \int dx \Delta g(x)$$

$$\sim 20\% (\text{with RHIC data})$$

Orbital Angular Momentum of quarks and gluons
Little known

Image courtesy of Jian-Wei Qiu

Quark model assumes spin of proton (1/2) equals spin of u+u+d,
but European Muon Collaboration (EMC) found quarks only contribute < 30%

How to access it?

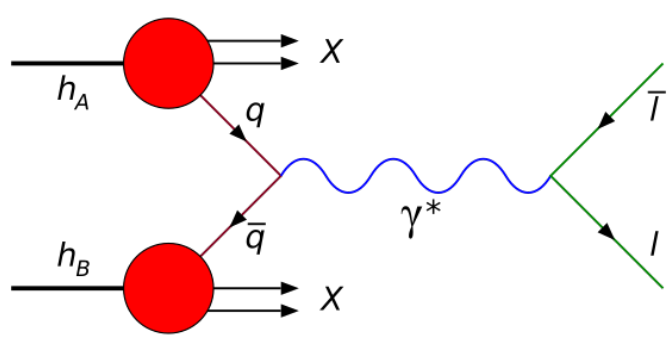

Drell-Yan

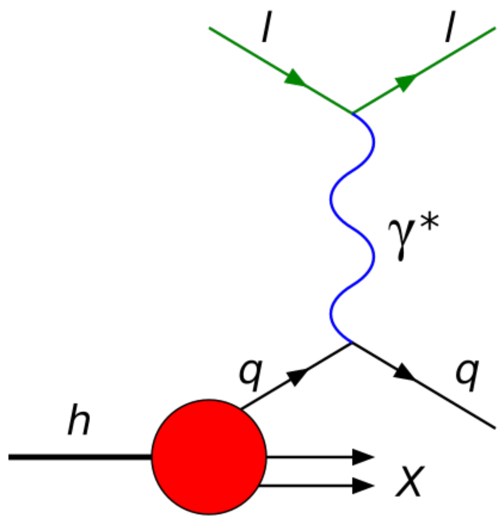

DIS

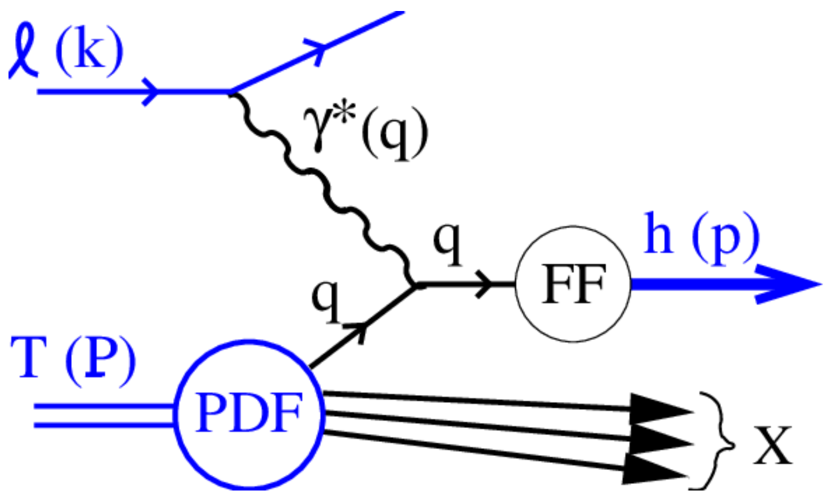

SIDIS

Measure structure functions (via longitudinal spin asymmetries) in processes like polarized lepton/hadron scattering off a polarized target proton

<u>Existing experimental efforts in last 3 decades:</u>
p-p collision at RHIC;
Open-charm muon production at COMPASS;
Neg./pos. pion/kaon production at HERMES…

Global analysis of the experimental data

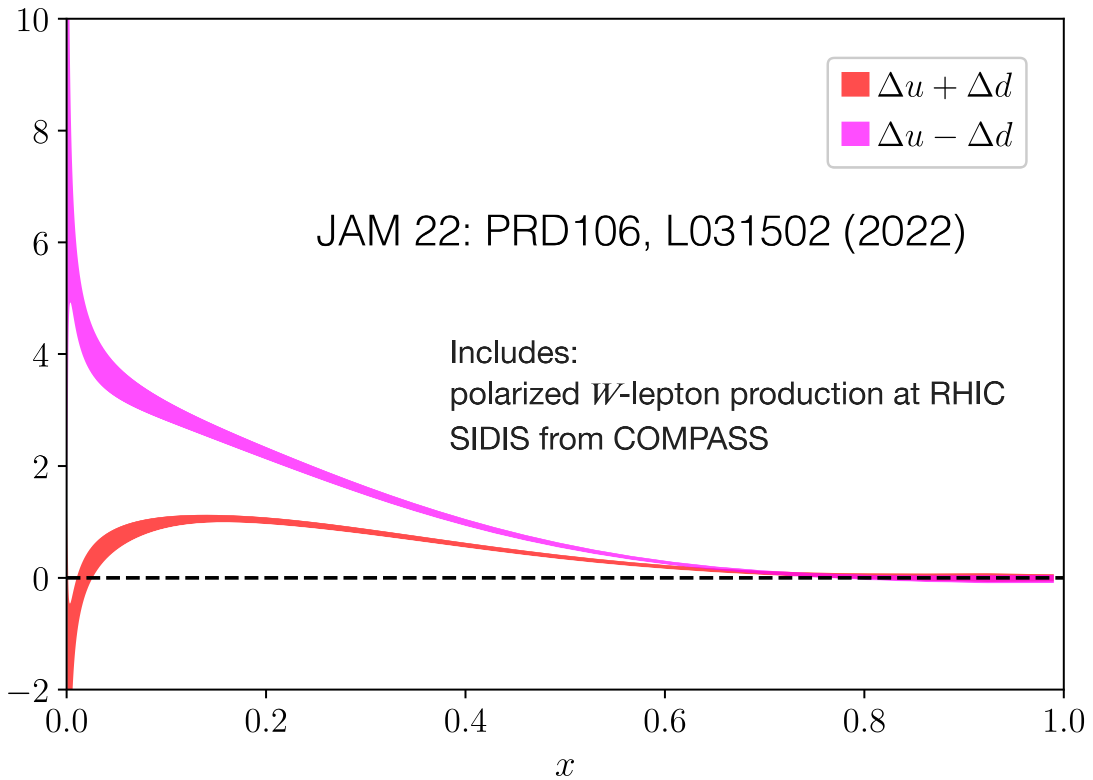

Why EIC?

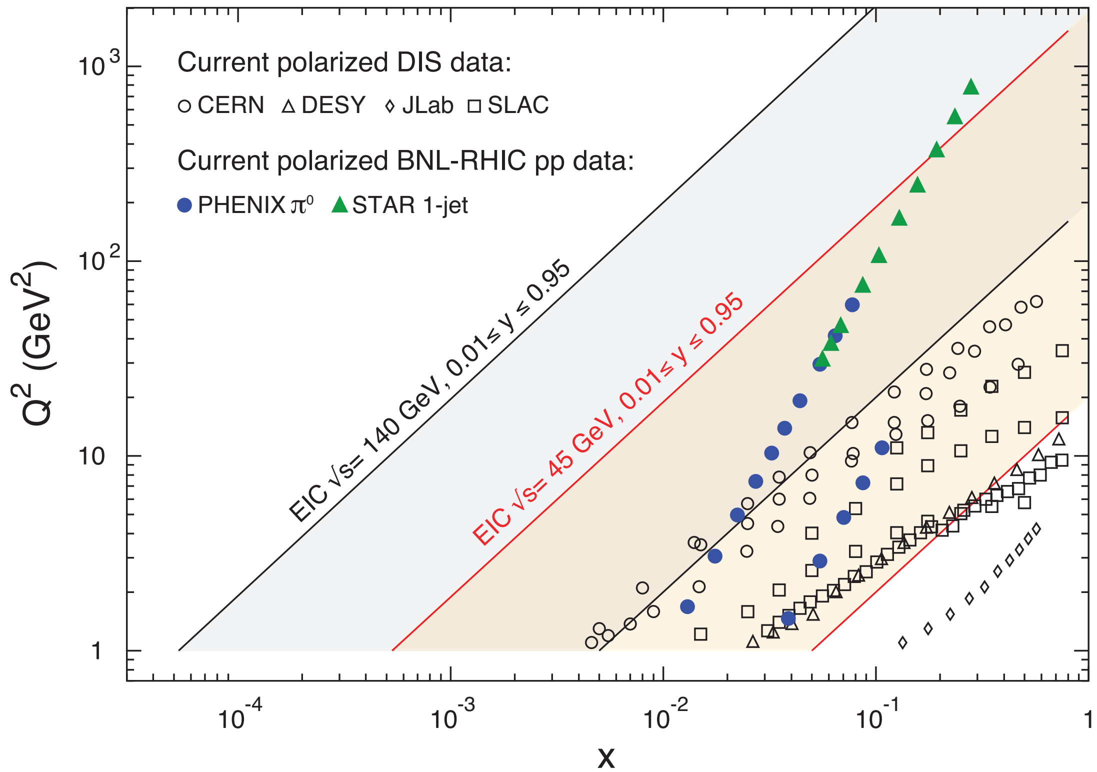

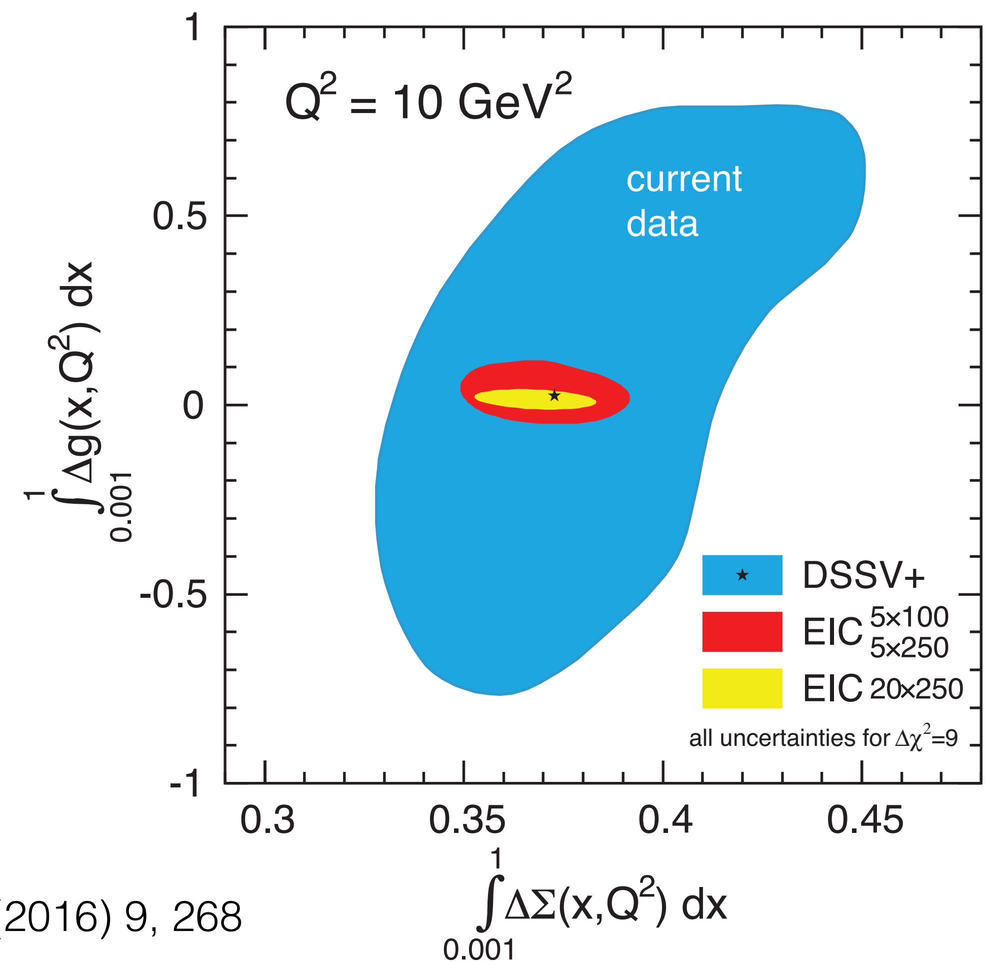

EIC White Paper: EPJA 52 (2016) 9, 268

- High luminosity provides more precise statistical measurements
- High polarization capacities of electron and nucleon give more access to the spin-dependent observables
- Unprecedented low-x reach for polarized DIS experiment

Status of lattice determinations

LQCD provides *ab initio* determination from first-principle!

	m_π [MeV]	a [fm]	P_z [GeV]
LP^3 Coll. 18$'$	physical	0.09	3.0
Gao, *et al.*, PRD20$'$	310	0.042	2.77
HadStruc Coll. 22$'$	358	0.094	2.5
Holligan and Lin, 24$'$	315	0	1.75
This work	physical	0.076	1.53

Having both continuum limit and physical mass limit is still challenging!

Outline

- Theoretical aspects
- Lattice techniques and setup
- Results via pseudo-PDF approach
  - Mellin moments
  - Light cone PDF
- Results via quasi-PDF approach
  - Light cone PDF
- Comparison with global fit results and discussions

All results are preliminary!

Matrix element corresponding to quark helicity

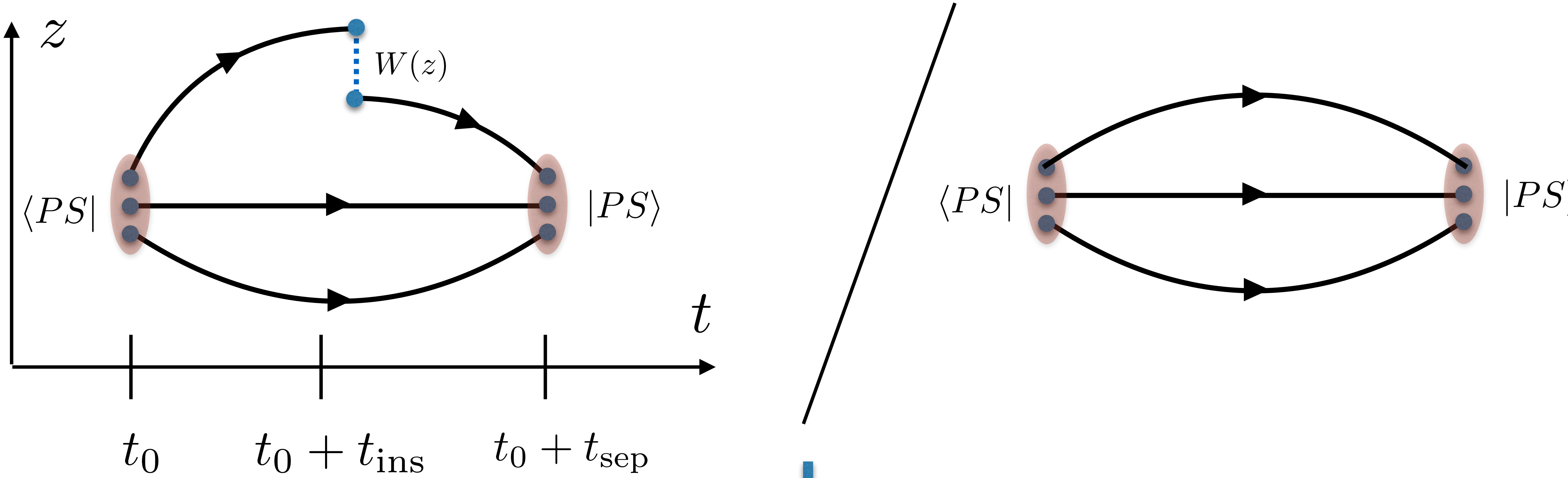

$0 \ll t_{\rm ins} \ll t_{\rm sep}$

Parton spin in z direction

$$h_B^f(z, P_z, a) = \left\langle PS|\bar{\psi}(z)\gamma_z\gamma_5 W(z,0)\psi(0)|PS\right\rangle$$

$f = u - d, u + d$

Both isovector and isoscalar sector
Ignore disconnected diagrams

$P_\mu = (P_0, 0, 0, P_z)$ Hadron momentum in z direction

Joint fit for the bare matrix element

$$R(t_{\text{ins}}, t_{\text{sep}}, P_z) = h_B(z, P_z) \frac{1 + c_1(z, P_z)(e^{-\Delta E t_{\text{ins}}} + e^{-\Delta E(t_{\text{sep}} - t_{\text{ins}})})}{1 + c_2 e^{-\Delta E t_{\text{sep}}}}$$

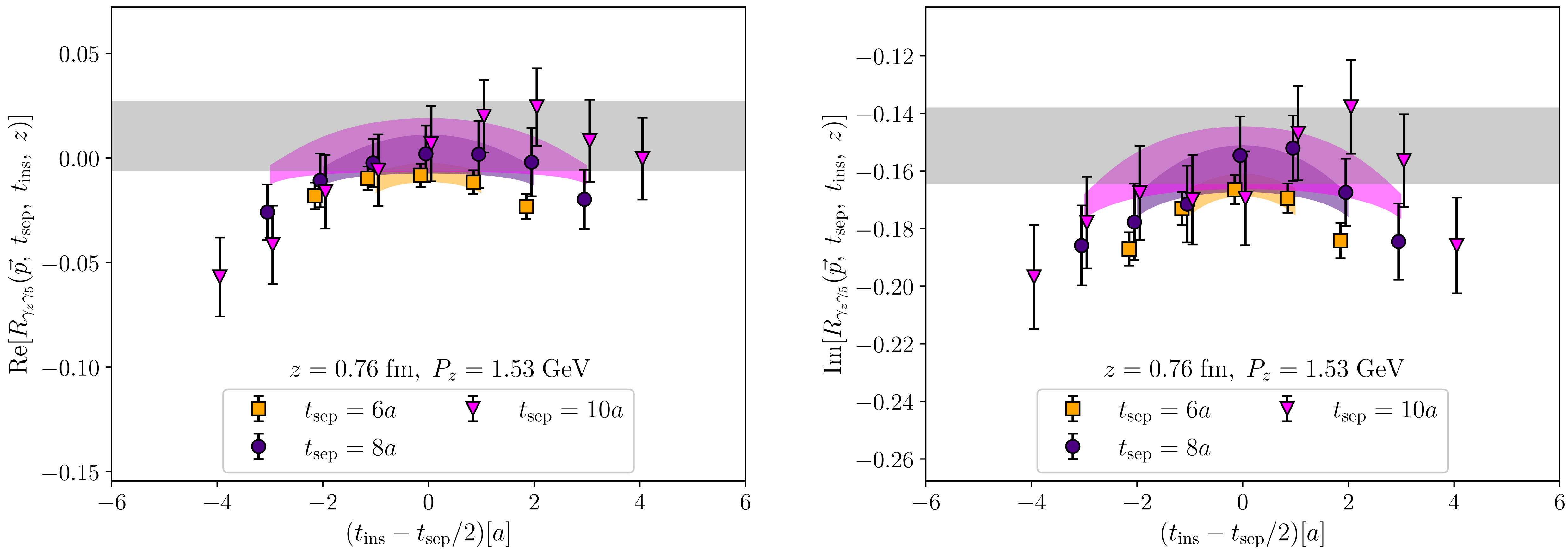

Good control of excited-state contamination

Joint fit v.s. summation method

$$S(t_{\text{sep}}, P_z, z, n_{\text{exc}}) = \sum_{t_{\text{ins}}=t_0+n_{\text{exc}}}^{t_{\text{sep}}-n_{\text{exc}}} R(t_{\text{ins}}, t_{\text{sep}}, P_z, z) = B_0 + t_{\text{sep}} h_B(z, P_z)$$

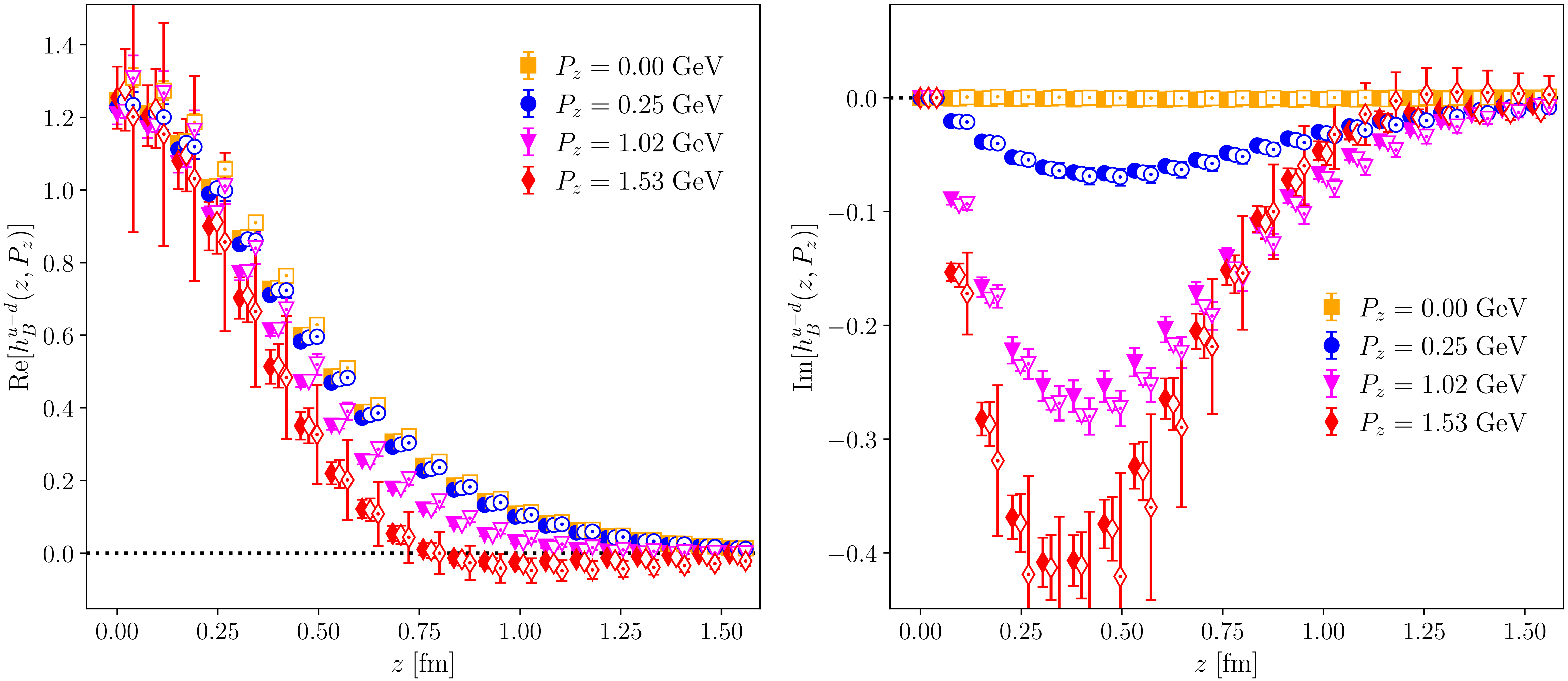

Filled points: joint fit using t_{sep}/a=[6,8,10]
Open points: summation method using t_{sep}/a=[6,8,10]
Open points with dot inside: summation method using t_{sep}/a=[8,10,12]

Consistent among different extraction strategies
Clear momentum dependence

Fit Mellin moments from reduced ITD

Operator product expansion (OPE) approximation inspired model:

$$\frac{h_B(z,P_z)}{h_B(z,P_z^0)}\frac{h_B(0,P_z^0)}{h_B(0,P_z)} = \mathcal{M}(\lambda, z^2, P_z^0) = \frac{\sum_{n=0} C_n(\mu^2 z^2)\frac{(-i\lambda)^n}{n!}\langle x^n\rangle(\mu)}{\sum_{n=0} C_0(\mu^2 z^2)\frac{(-i\lambda_0)^n}{n!}\langle x^n\rangle(\mu)} + \mathcal{O}(\Lambda_{\mathrm{QCD}}^2 z^2)$$

Lattice data as input (points)

Mellin moments as fit parameters (bands)

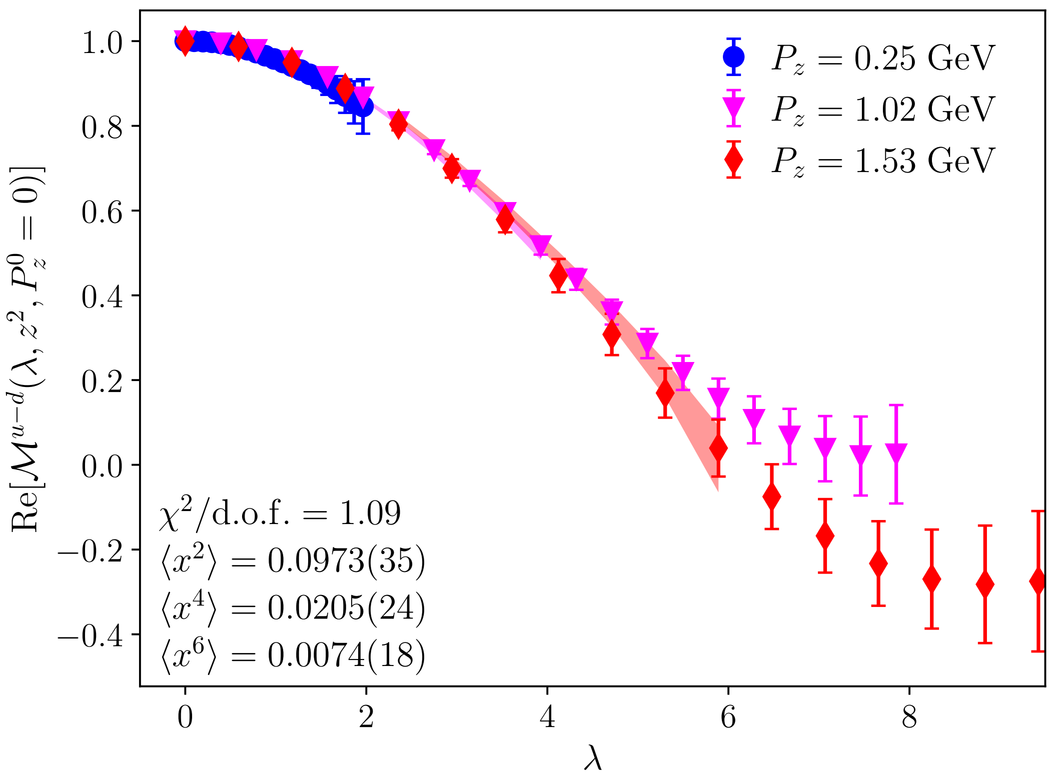

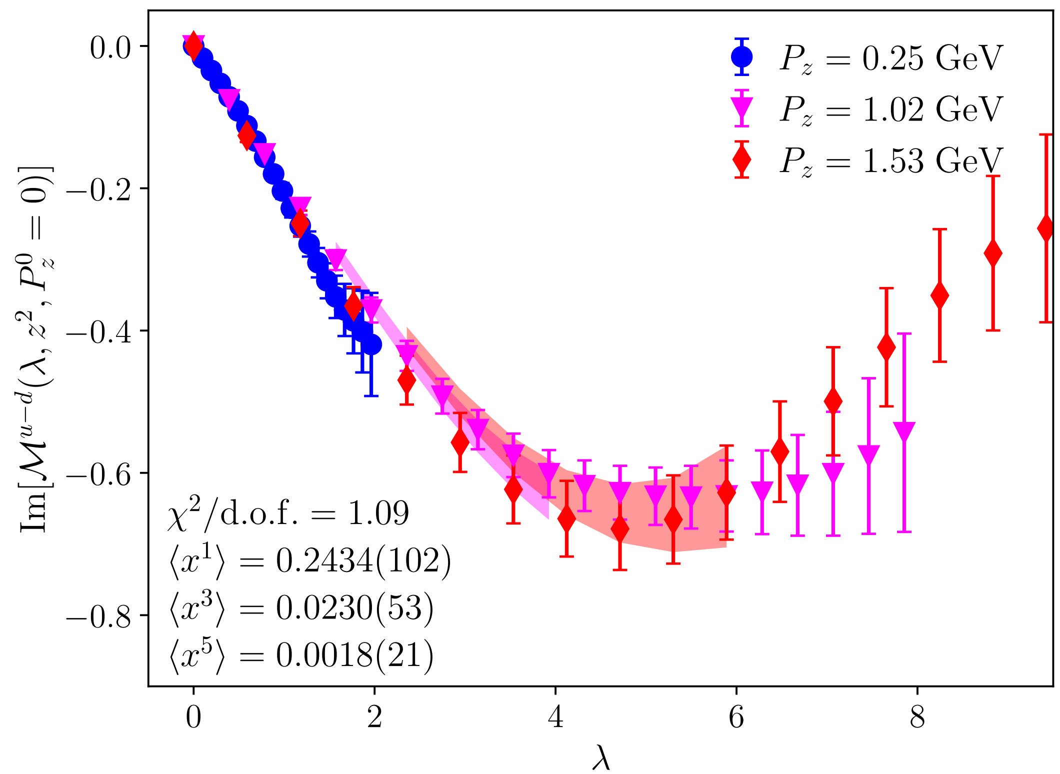

Including first 6 Mellin moments describes the data well
Controlled precision for the first 2 moments

Compare to global fit results

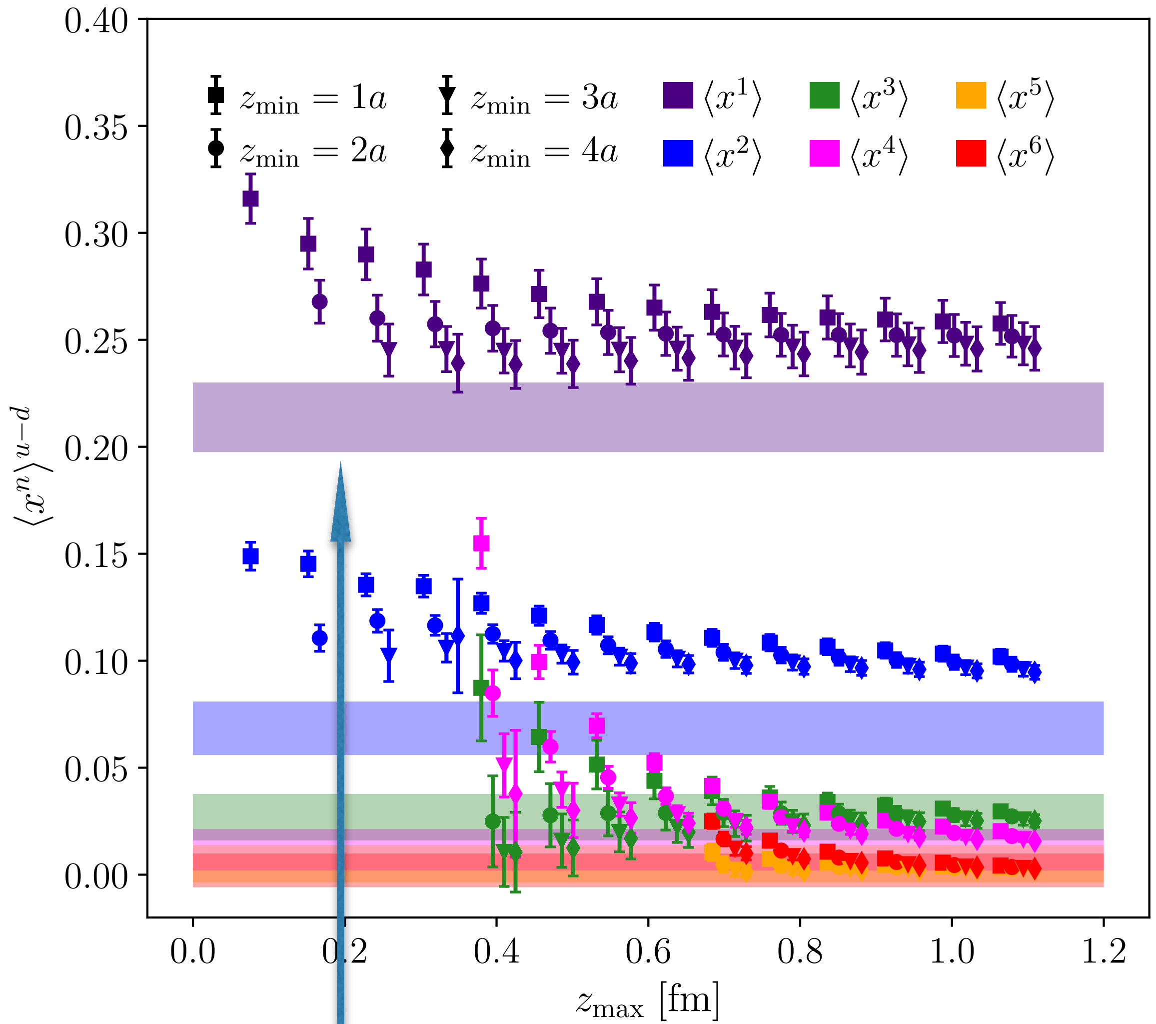

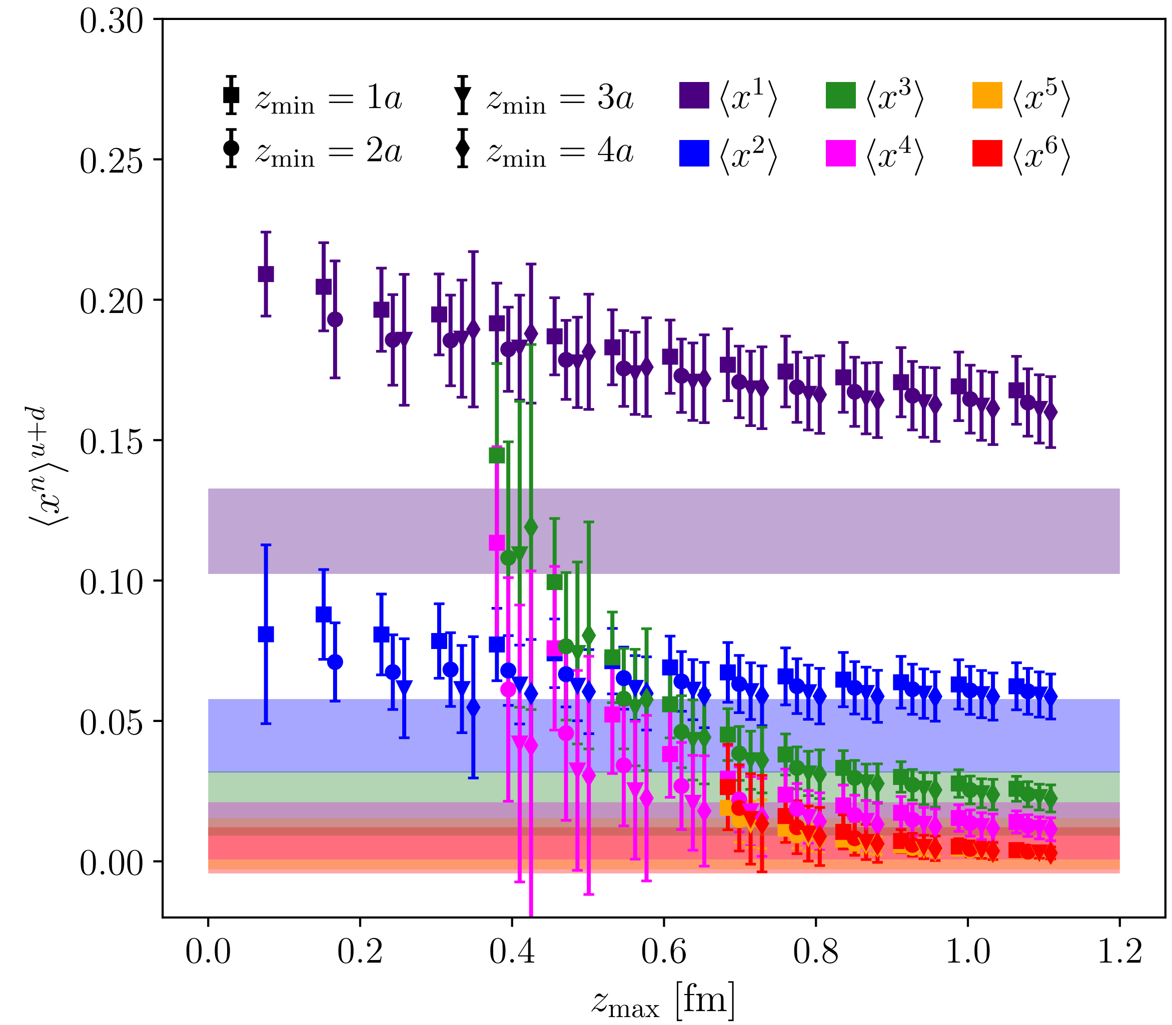

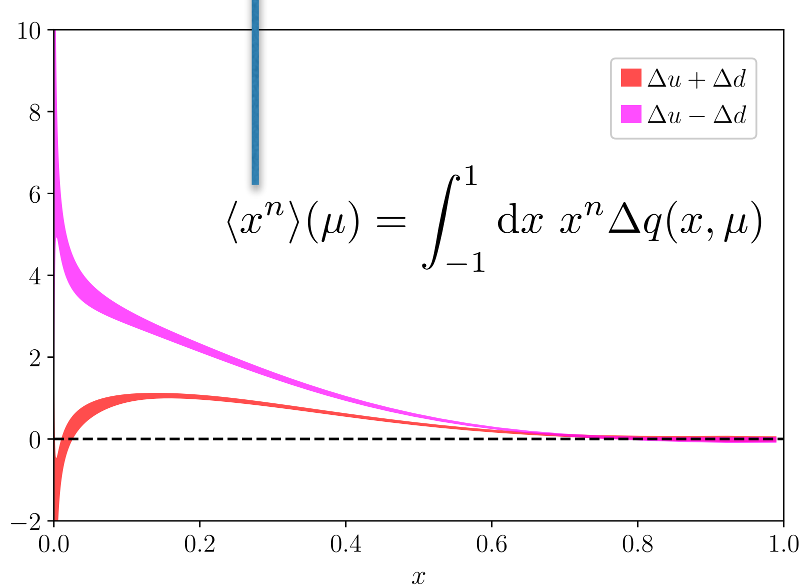

Stable results when using different data sets
Larger than JAM 22 results by 1-2σ

Light cone PDF from reduced ITD using DNN

$$\mathcal{M}_{\rm DNN}(z, P_z, \mu, P_z^0 = 0) = \int_{-1}^{1} d\alpha \, \frac{\mathcal{C}(\alpha, \mu^2 z^2)}{C_0(\mu^2 z^2)} \int_0^1 dx \, e^{-ix\alpha\lambda} \Delta q(x, \mu) = \int_0^1 dx \, \Delta q(x, \mu) \bar{\mathcal{C}}(x\lambda, \mu^2 z^2)$$

Input data

Target solution as output

Known convolution kernel

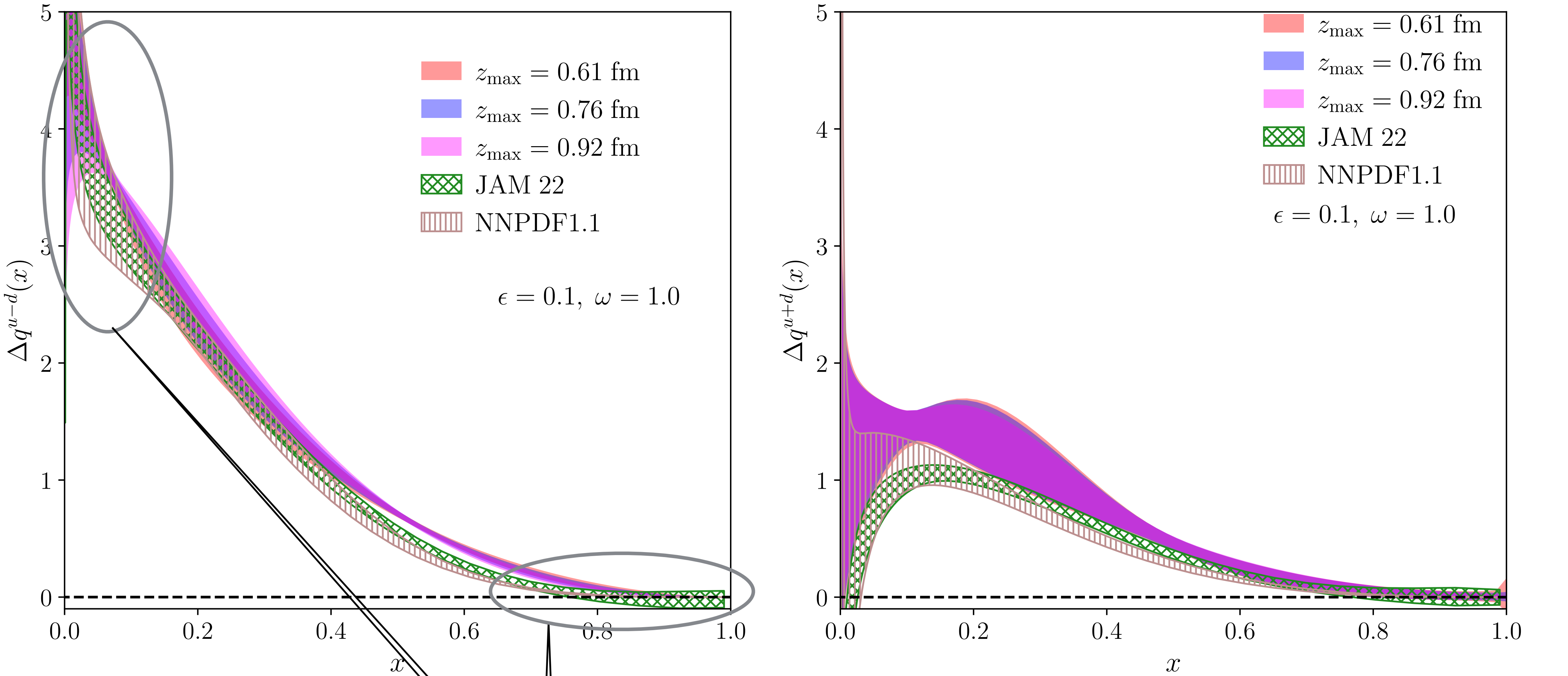

$$\Delta q(x) = A x^{\alpha} (1 - x)^{\beta} [1 + \epsilon \sin(f_{\rm DNN}(x, \boldsymbol{\theta}))]$$

Light cone PDF from reduced ITD using DNN

Stable results when fit with different data sets or regularization parameters
Good agreement with global analysis JAM 22 and NNPDF1.1 at moderate x

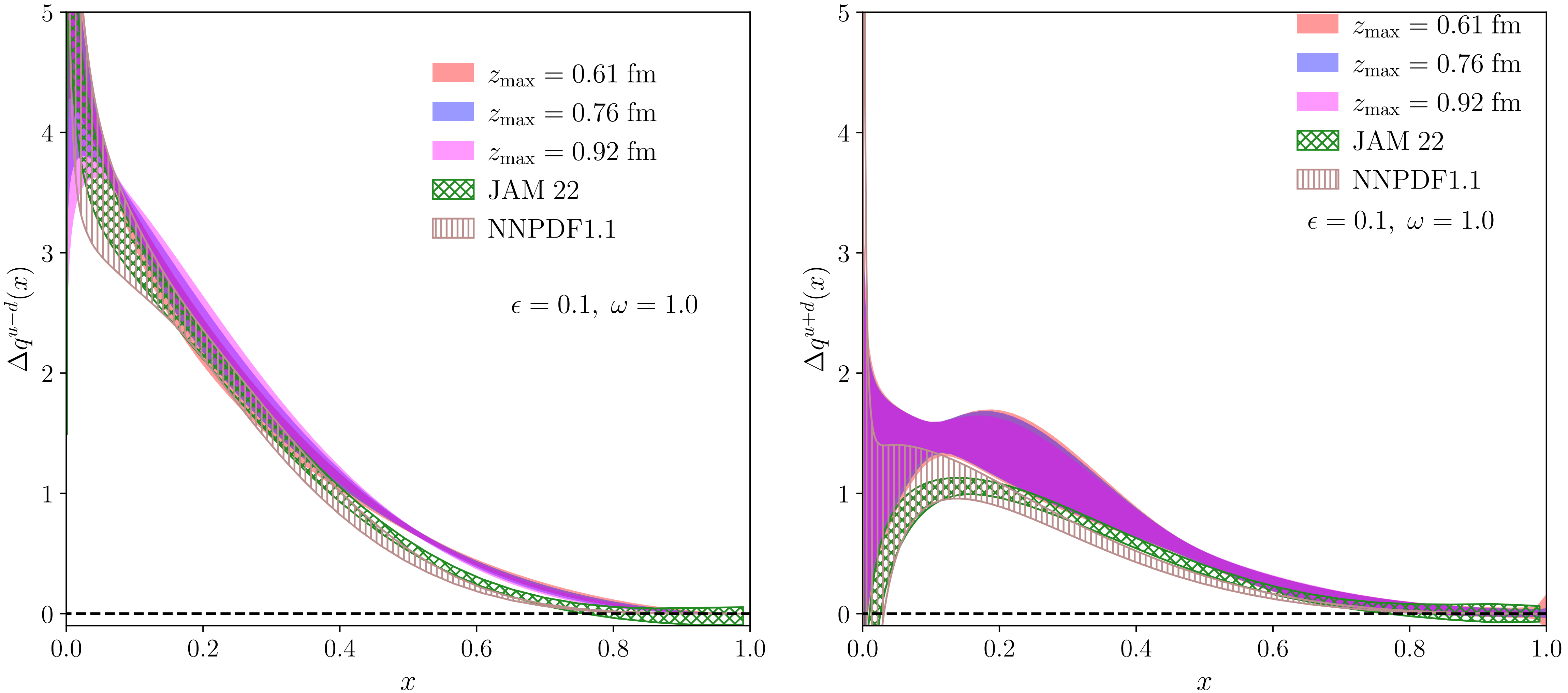

DNN fitted reduced ITD

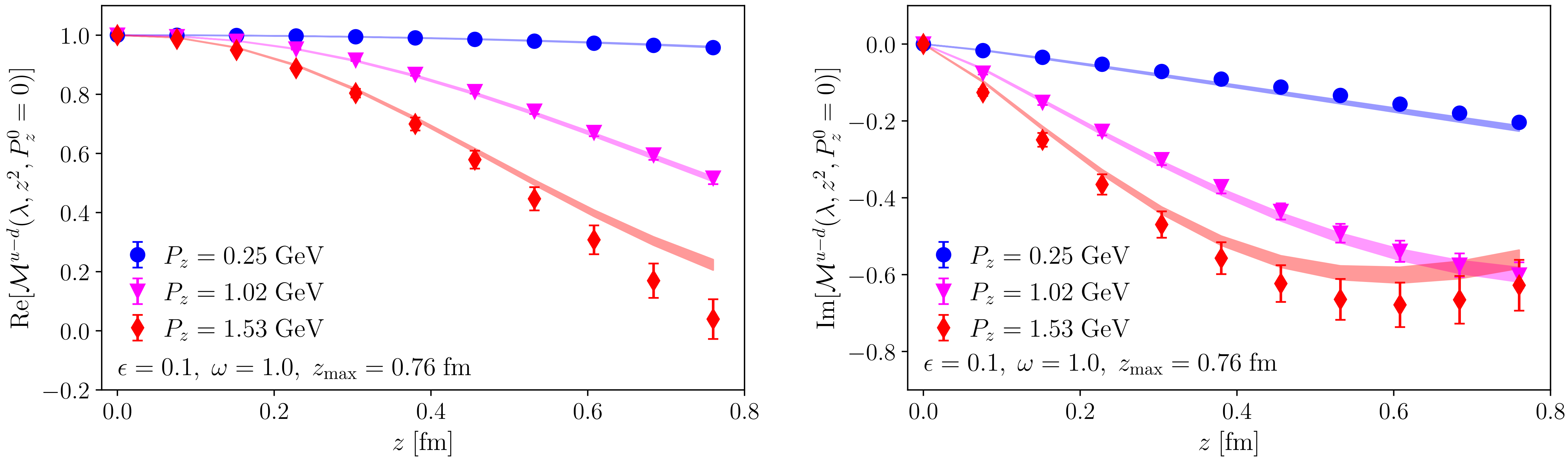

DNN fits dominated by data at small momentum
Slight tension between small momentum and large momentum

Quasi-PDF method: Hybrid scheme renorm.

$$h_R(z,P_z) = \begin{cases} \dfrac{h_B(z,P_z,a)}{h_B(z,P_z=0,a)} & |z| \le z_s \quad \text{Ratio scheme renorm.} \\ \dfrac{h_B(z,P_z,a)}{h_B(z_s,P_z=0,a)} e^{(\delta m+\bar{m}_0)(z-z_s)} & |z| \ge z_s \quad \text{Self renorm.} \end{cases}$$

Other renormalizations distort IR behavior of the bi-local operator at large z!

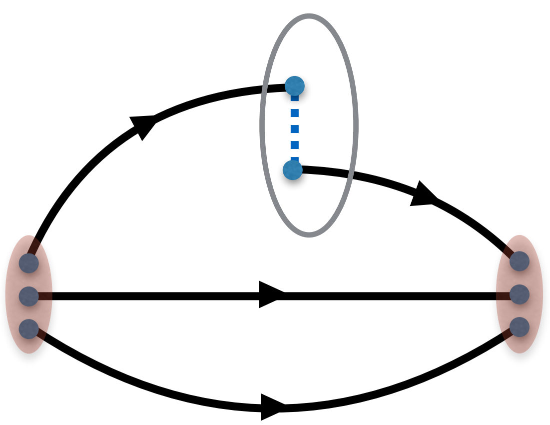

Multiplicative renormalization:

$$h_B(z,P_z) = Z_A e^{-\delta m\cdot z} e^{-\bar{m}_0\cdot z} h_R(z,P_z)$$

- Z_A: log. divergence from quark-WL vertex
- $e^{-\delta m\cdot z}$: Linear divergence from WL self-energy
- $e^{-\bar{m}_0\cdot z}$: Renomalon from scheme-dependence of delta*m

fixing to $\overline{\text{MS}}$ scheme : $h(z,P_z=0) \to C_0$

$$\frac{h_B(z,P_z,a)}{h_B(z-a,P_z,a)} e^{a\delta m} = e^{-a\bar{m}_0} \frac{C'_{0,\text{PV}}(\alpha_s(2\kappa e^{-\gamma_E}/z))}{C'_{0,\text{PV}}(\alpha_s(2\kappa e^{-\gamma_E}/(z-a)))} e^{K(2\kappa e^{-\gamma_E}/z,\, 2\kappa e^{-\gamma_E}/(z-a))}$$

$C_0 \to C'_0$: LRR the logs for $\bar{m}_0$

RGR : $\mu = 2$ GeV $\to \mu = 2\kappa e^{-\gamma_E}/z$

Quasi-PDF method: determination of renormalon

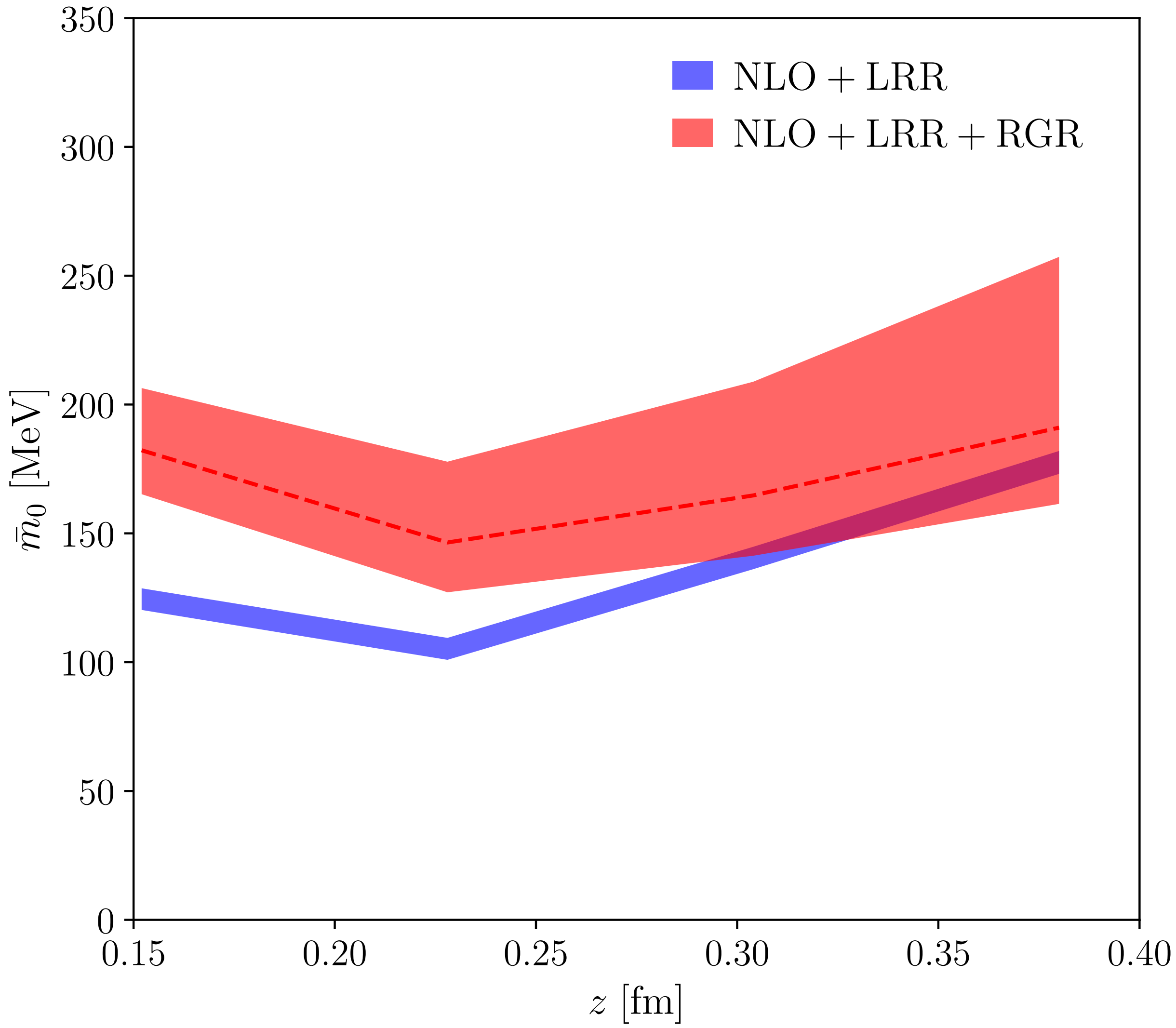

Plateau ~ z = 3a: controlled discretization effects and high twist effects

$$h_R(z, P_z) = \begin{cases} \frac{h_B(z,P_z,a)}{h_B(z,P_z=0,a)} & |z| \leq z_s \\ \frac{h_B(z,P_z,a)}{h_B(z_s,P_z=0,a)} e^{(\delta m+\bar{m}_0)(z-z_s)} & |z| \geq z_s \end{cases}$$

Renormalized matrix elements in Hybrid scheme

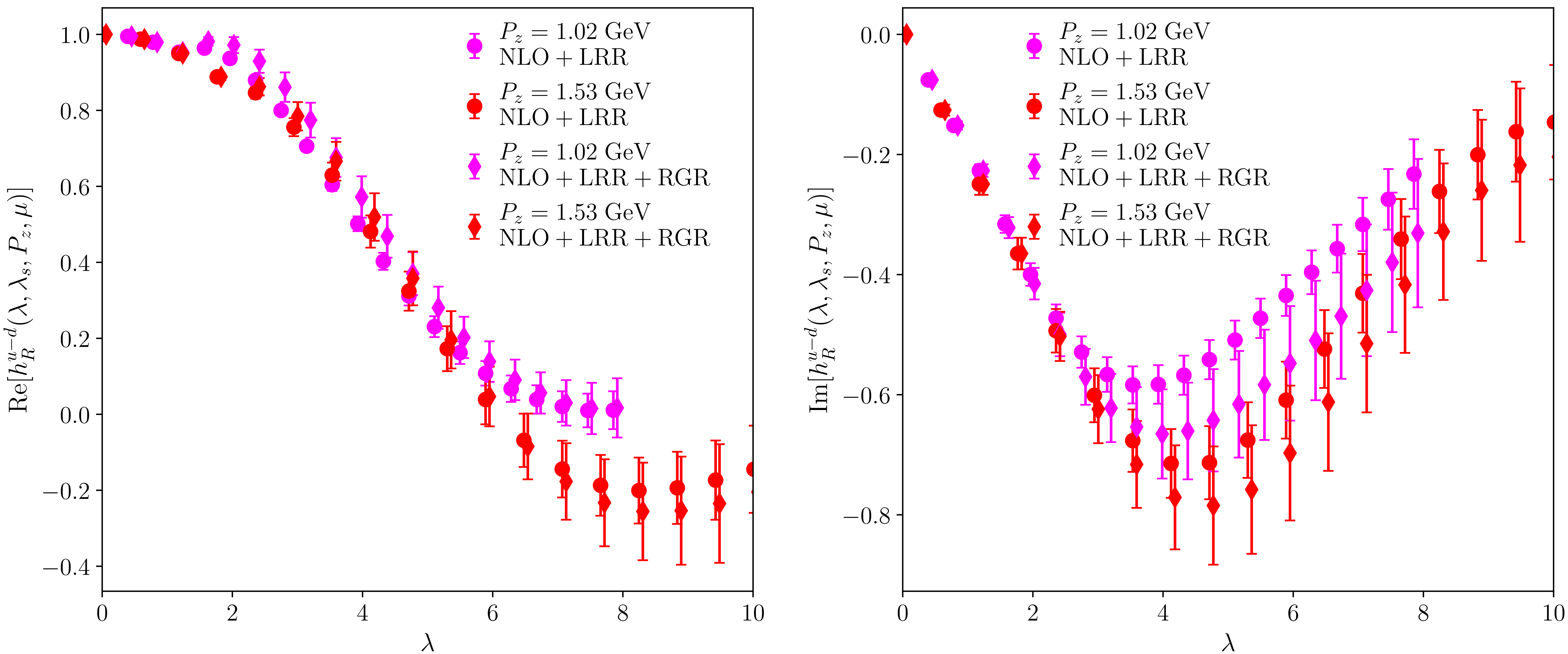

RGR introduces a small correction within 1σ statistical error
Larger error size when with RGR, from scale variation
Visible momentum dependence

Large lambda extrapolation

$$h_R^{\mathrm{extra}}(\lambda, \lambda_s, P_z, \mu) = \frac{A e^{-m_{\mathrm{eff}}\lambda/P_z}}{|\lambda|^d}$$

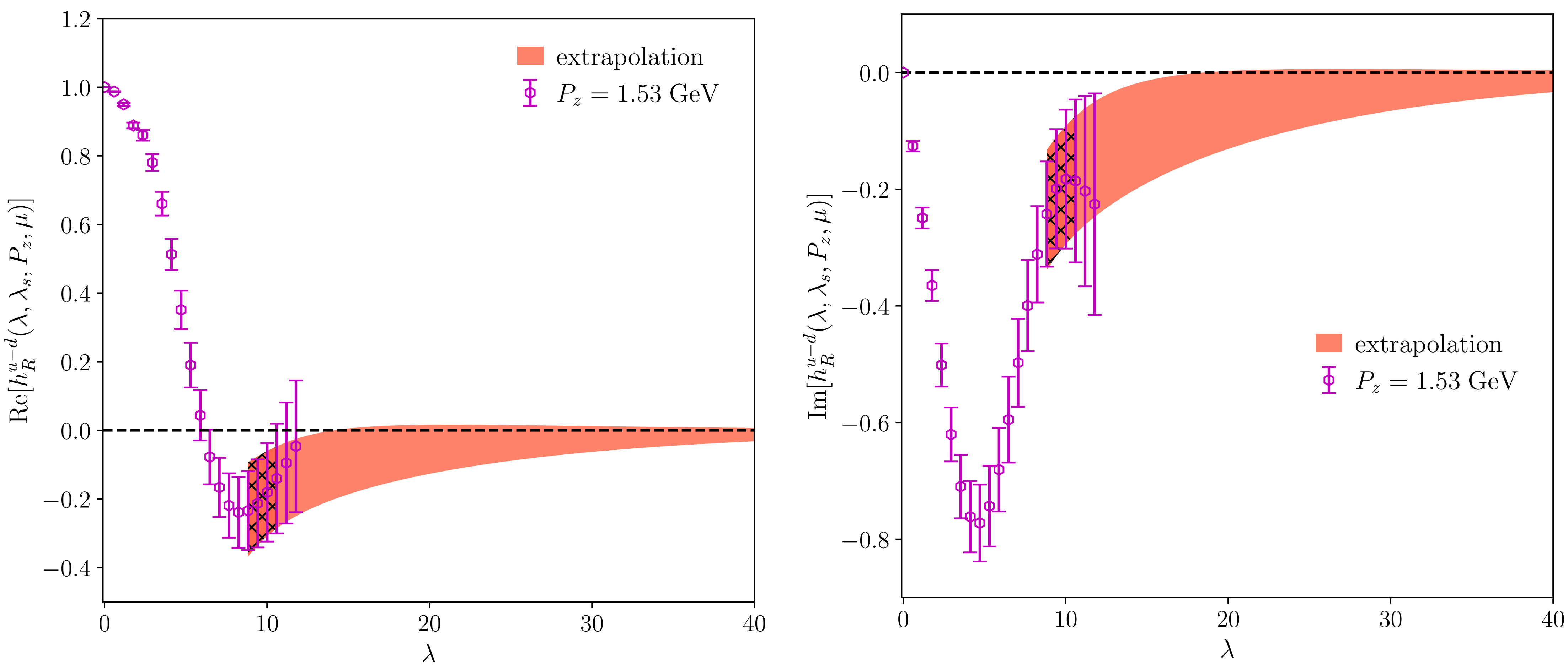

$$\Delta\tilde{q}(y,\mu) = \int \frac{\mathrm{d}\lambda}{2\pi} e^{iy\lambda} h_R(\lambda, \lambda_s, P_z, \mu)$$ ⟶ Quasi-PDF

quasi-PDF in x-space

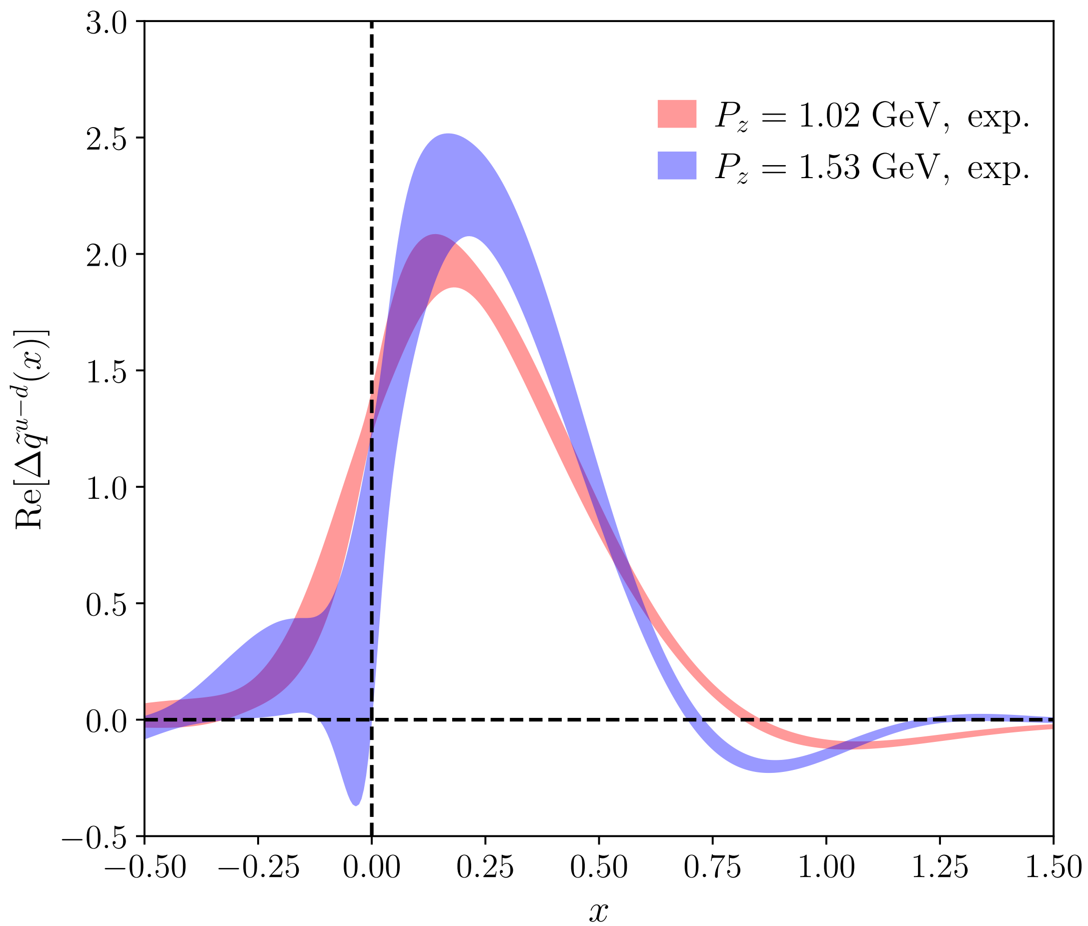

NLO+LRR

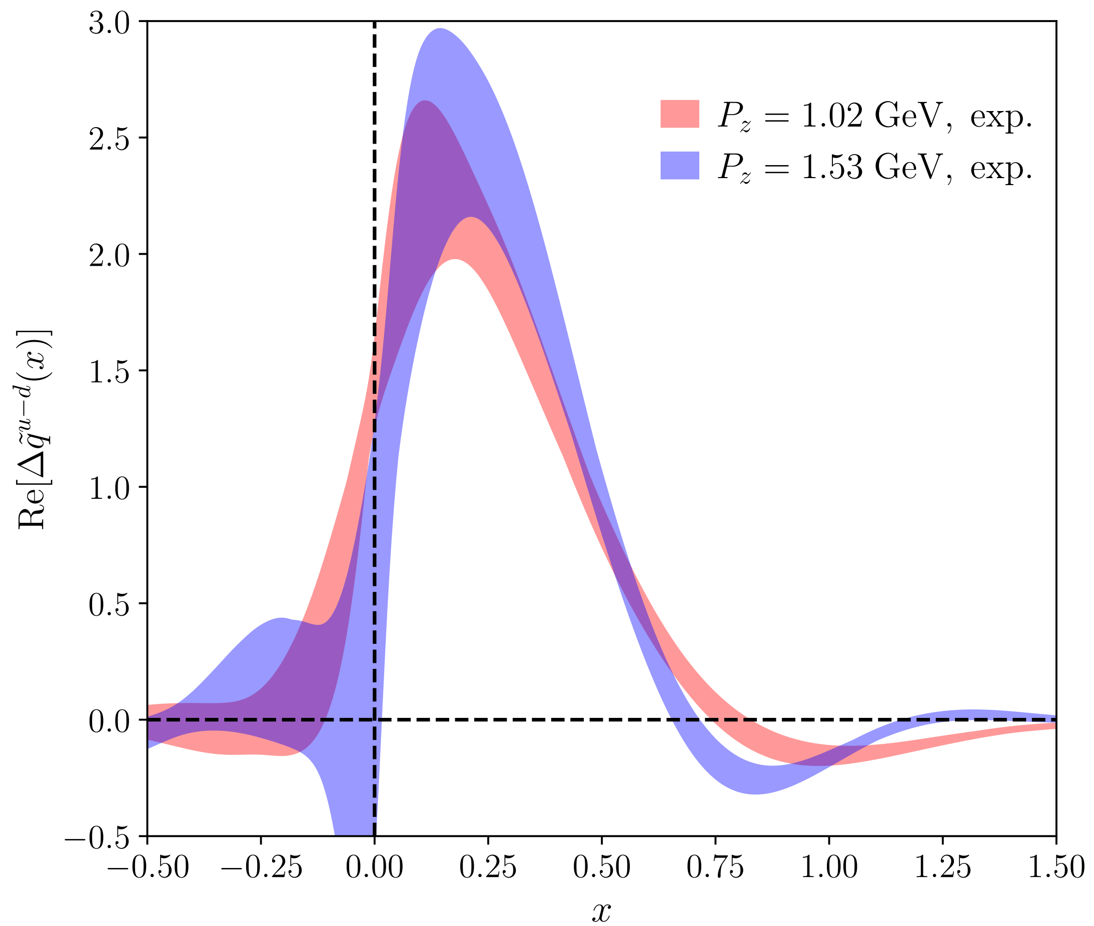

NLO+LRR+RGR

Imaginary parts are zero within errors
Visible momentum dependence
RGR induces a small enhancement and the error grows

Perturbative matching

$$\Delta q(x,\mu) = \int_{-\infty}^{+\infty} \frac{\mathrm{d}y}{|y|}\, \mathcal{C}^{-1}\left(\frac{x}{y},\mu,z_s,P_z\right) \Delta\tilde{q}(y,\mu) + \mathcal{O}\left(\frac{\Lambda^2_{\mathrm{QCD}}}{(xP_z)^2}, \frac{\Lambda^2_{\mathrm{QCD}}}{\left((1-x)P_z\right)^2}\right)$$

Taylor expansion: $\mathcal{C}^{-1}\left(\frac{x}{y},\mu,z_s,P_z\right) = \delta\left(\frac{x}{y}-1\right) - \alpha_s \mathcal{C}^{(1)}\left(\frac{x}{y},\mu,z_s,P_z\right) + \mathcal{O}(\alpha_s^2)$

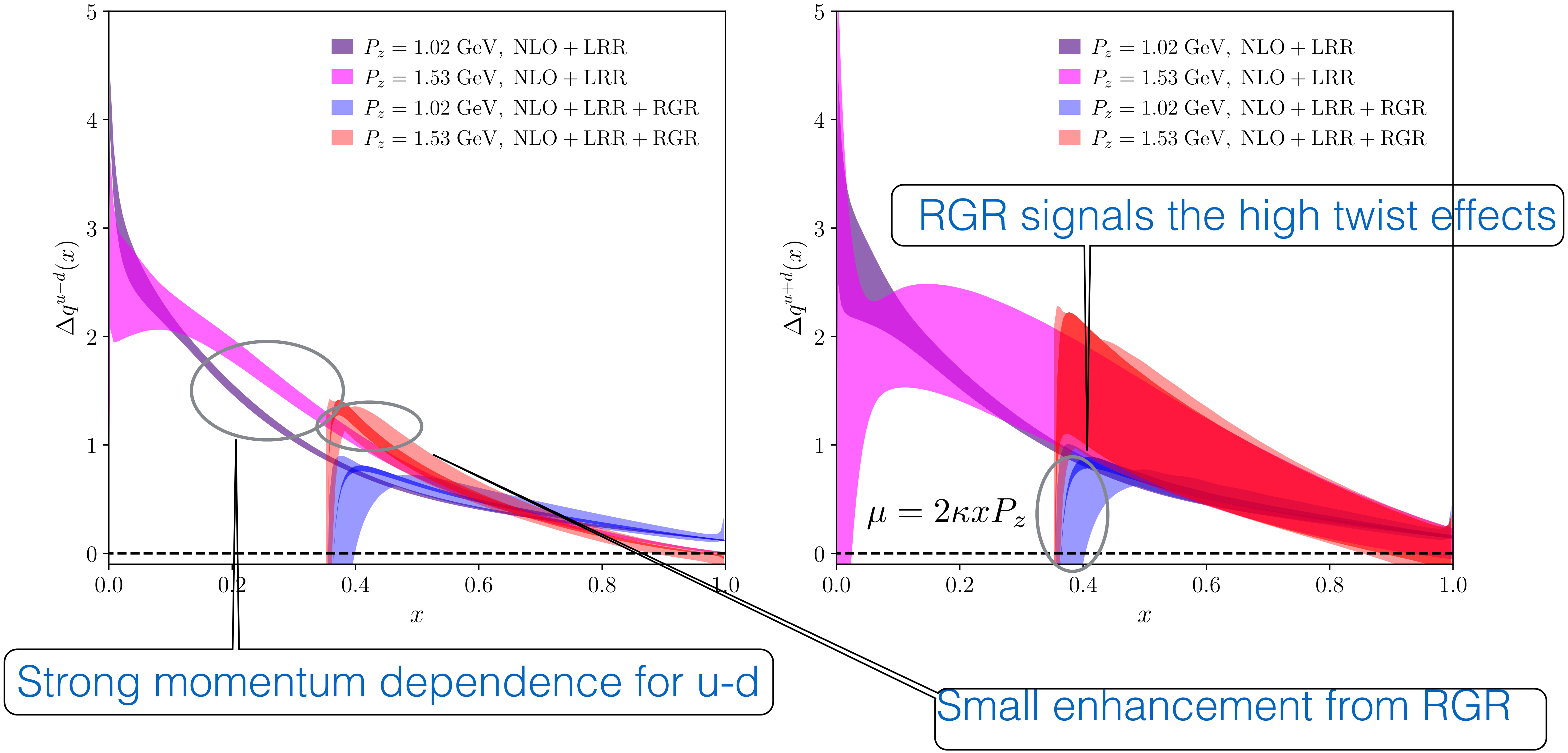

Complete comparison

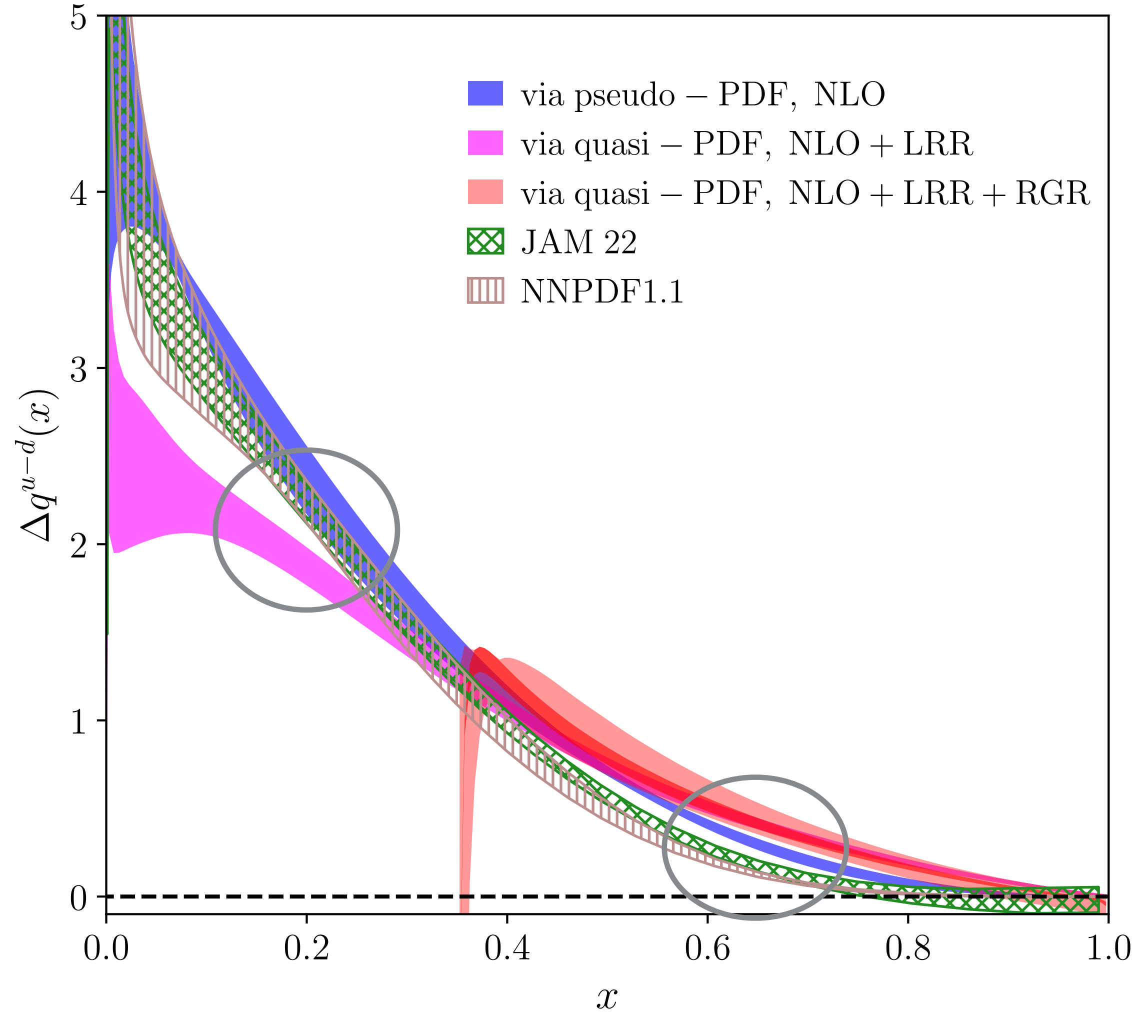

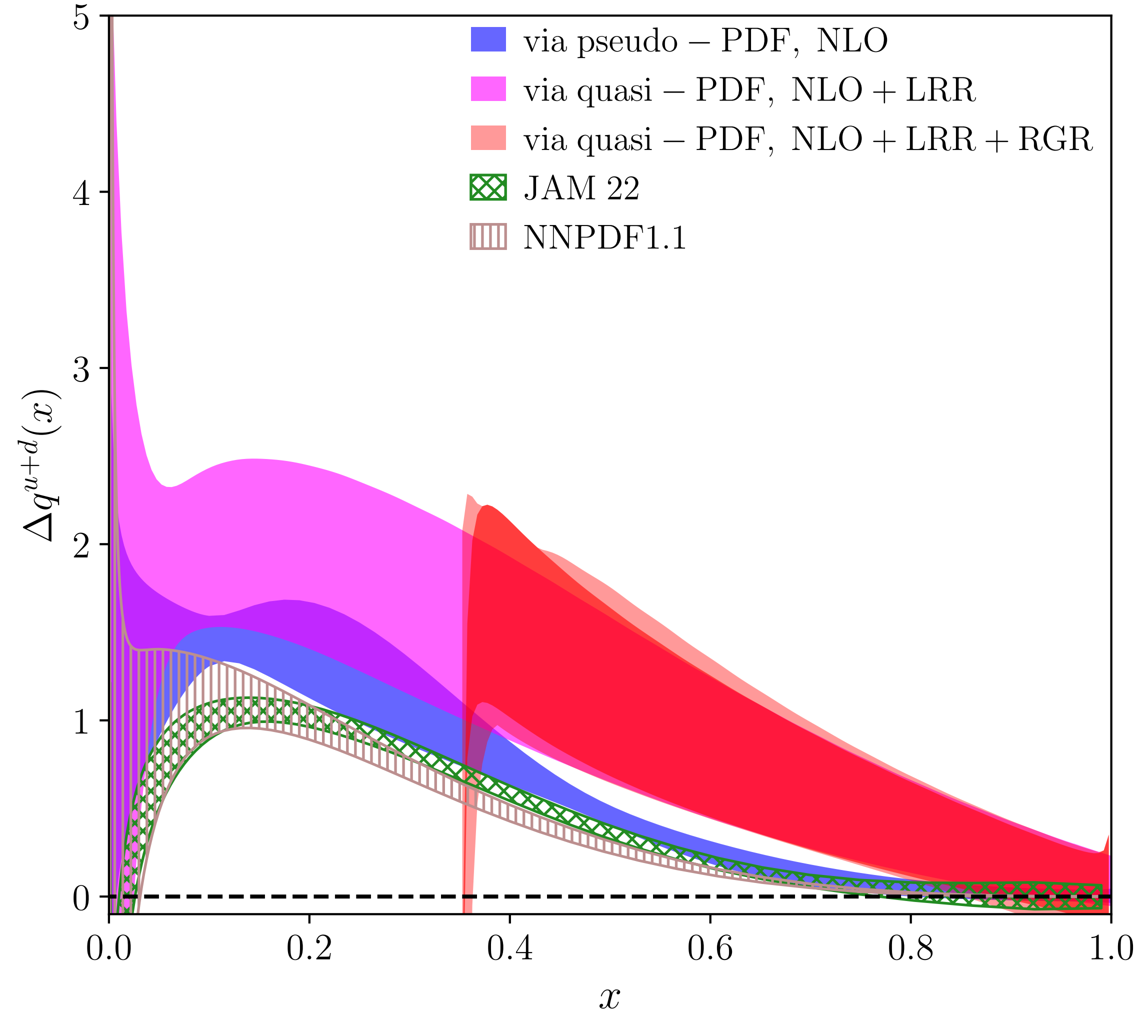

Visible difference between pseudo-PDF approach and quasi-PDF approach
Better agreement with global fit results for pseudo-PDF approach than quasi-PDF approach (need to investigate further)

Soffer bound (I)

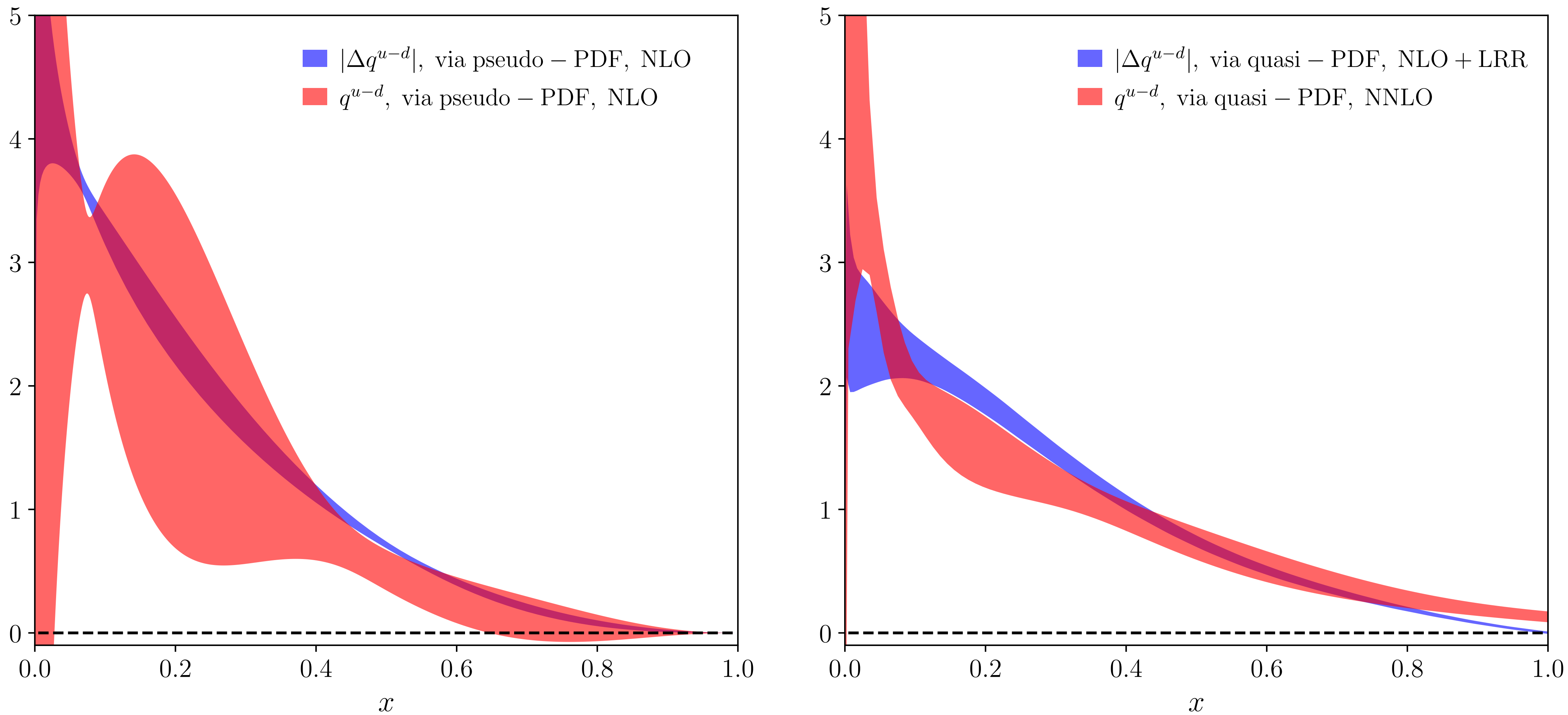

[J. Soffer, PRL 74, 1292 (1995)]

$$q(x) \geq |\Delta q(x)|$$

Soffer bound I respected within error

Soffer bound (II)

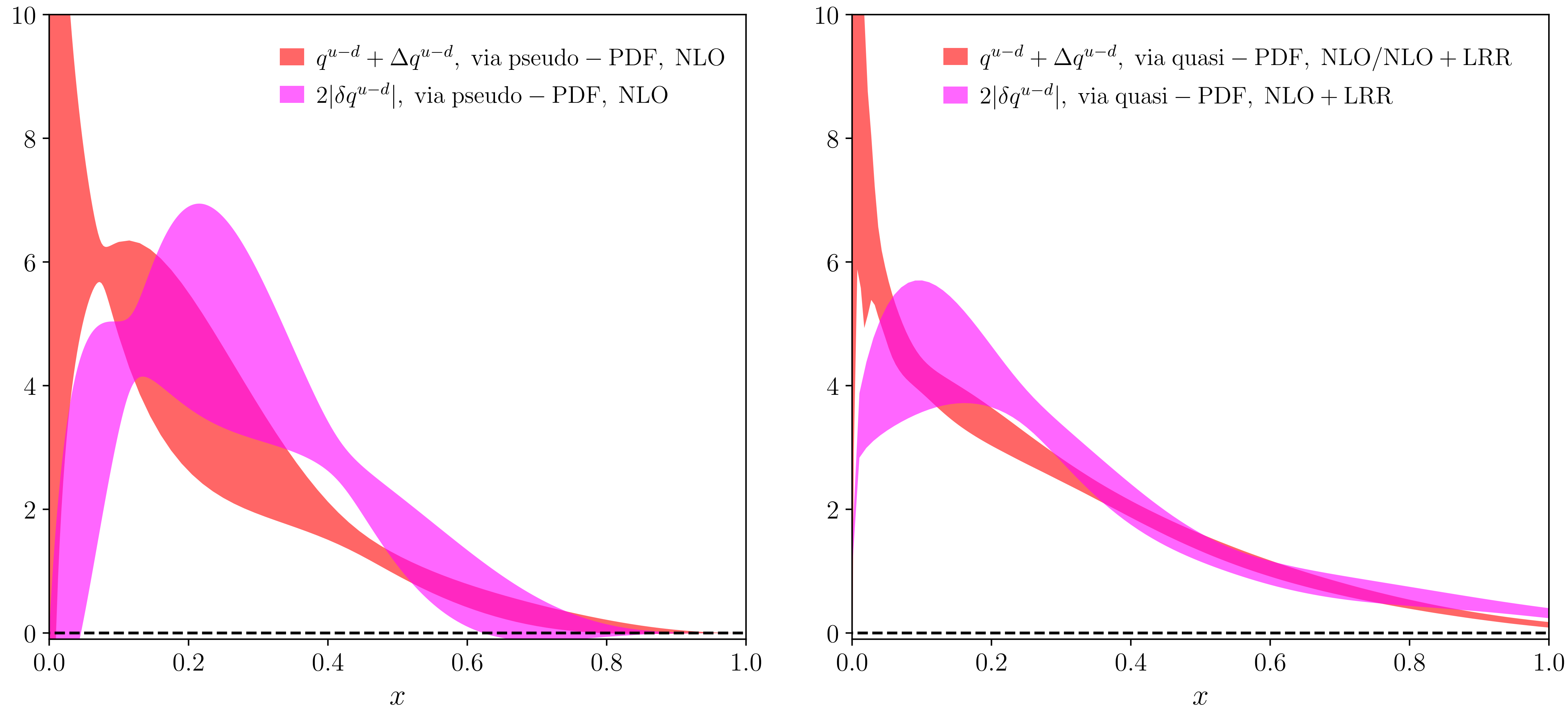

[J. Soffer, PRL 74, 1292 (1995)]

$$q(x) + \Delta q(x) \geq 2|\delta q(x)|$$

Soffer bound II not violated by 1-2σ

Conclusion

- ☑ Computed quark helicity matrix elements for both the isoscalar & isovector sectors
- ☑ Computed the Mellin moments (controlled precision for the first two)
- ☑ Computed the light cone PDF using both pseudo-PDF and quasi-PDF approach
- ☑ Adopted advanced reconstruction technique in the pseudo-PDF approach and state-of-the-art renormalization in the quasi-PDF approach
- ☑ Studied various systematics
- ☑ Examined the Soffer bound

- ☐ Push to larger momentum to suppress the high-twist effects
- ☐ Add more statistics to control the statistical uncertainties
- ☐ Add more lattice spacings for the continuum limit

Backup: Lattice setup

Ensembles $a, L_t \times L_s^3$	m_π (GeV)	N_{cfg}	n_z	k_z	t_{sep}/a	(#ex,#sl)
$a = 0.076$ fm 64×64^3	0.14	350	0	0	6	(1, 16)
			0	0	8,10	(1, 32)
			0	0	12	(2, 64)
			1	0	6,8,10,12	(1, 32)
			4	2	6	(1, 32)
			4	2	8,10,12	(4, 128)
			6	3	6	(1, 20)
			6	3	8	(4, 100)
			6	3	10,12	(5, 140)

Clover-wilson valence on HISQ sea

Momentum smearing to improve SNR

Backup: Sanity check of the joint fit

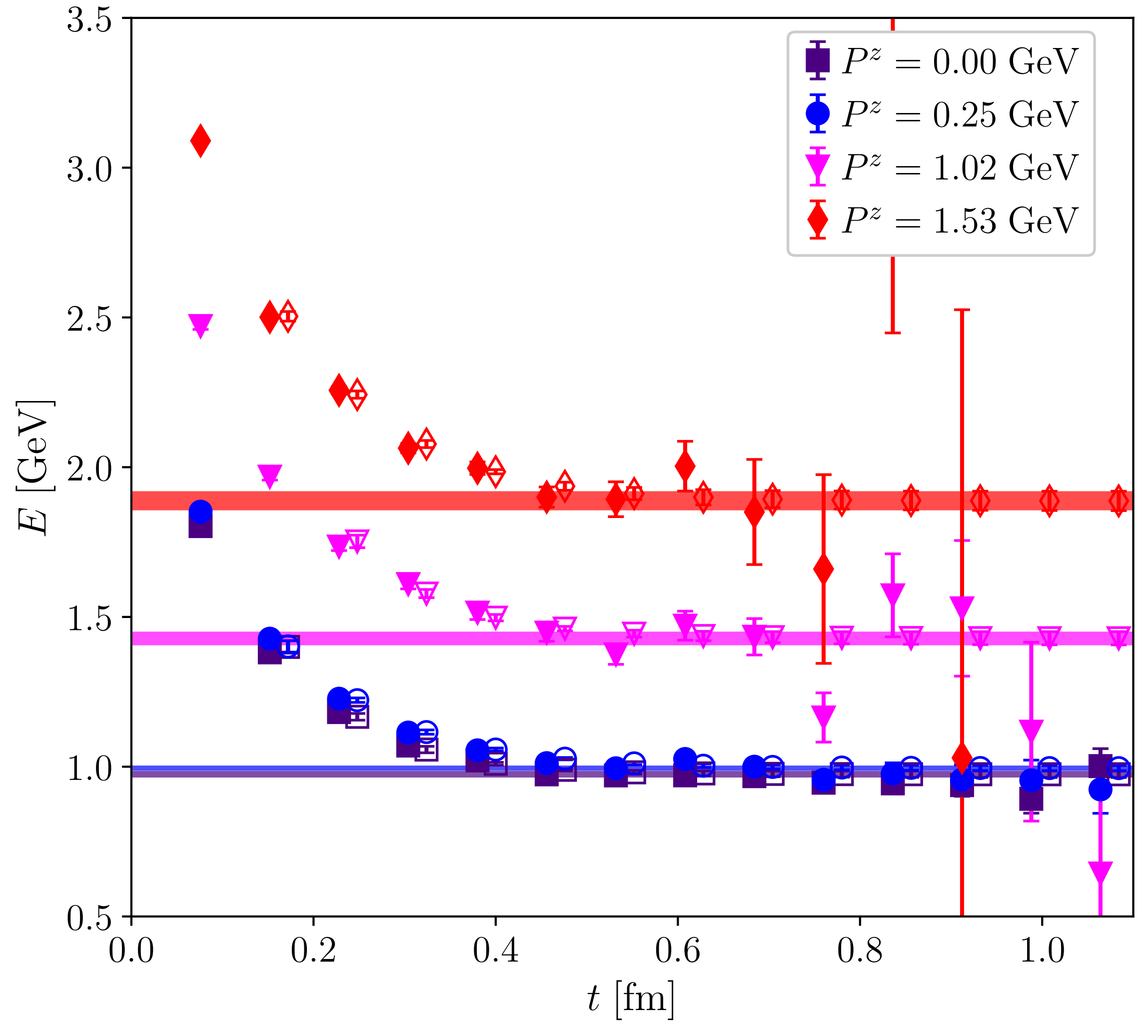

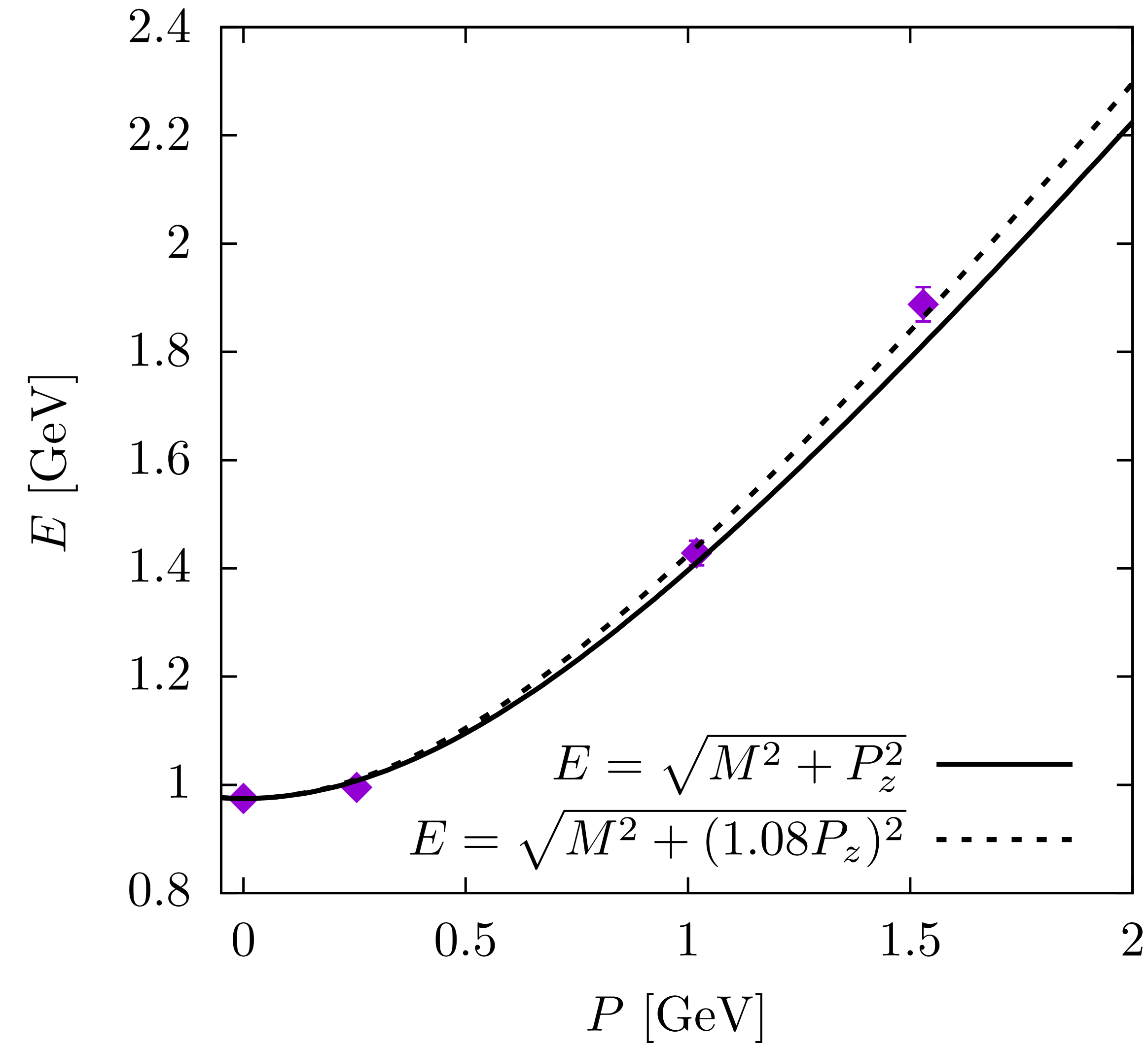

Filled points: effective mass from 2pt
Open points: effective mass from jointly-fit 2pt
Bands: ground-state mass from joint fit of R and 2pt

Good control of lattice discretization effects

Backup:

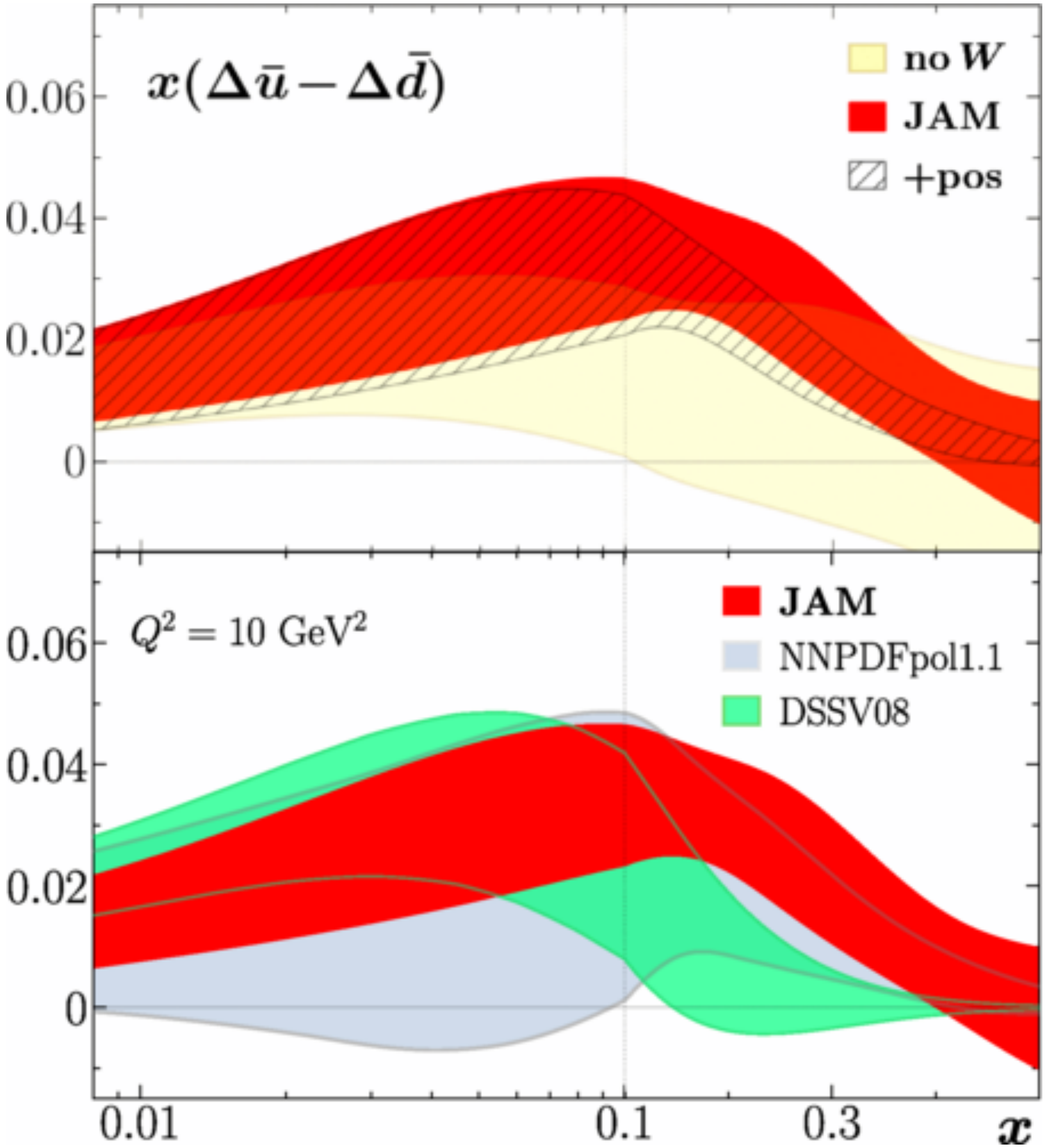

JAM 22: PRD106, L031502 (2022)

Non-zero contribution to spin from antiquarks

Renormalized axial-vector charge

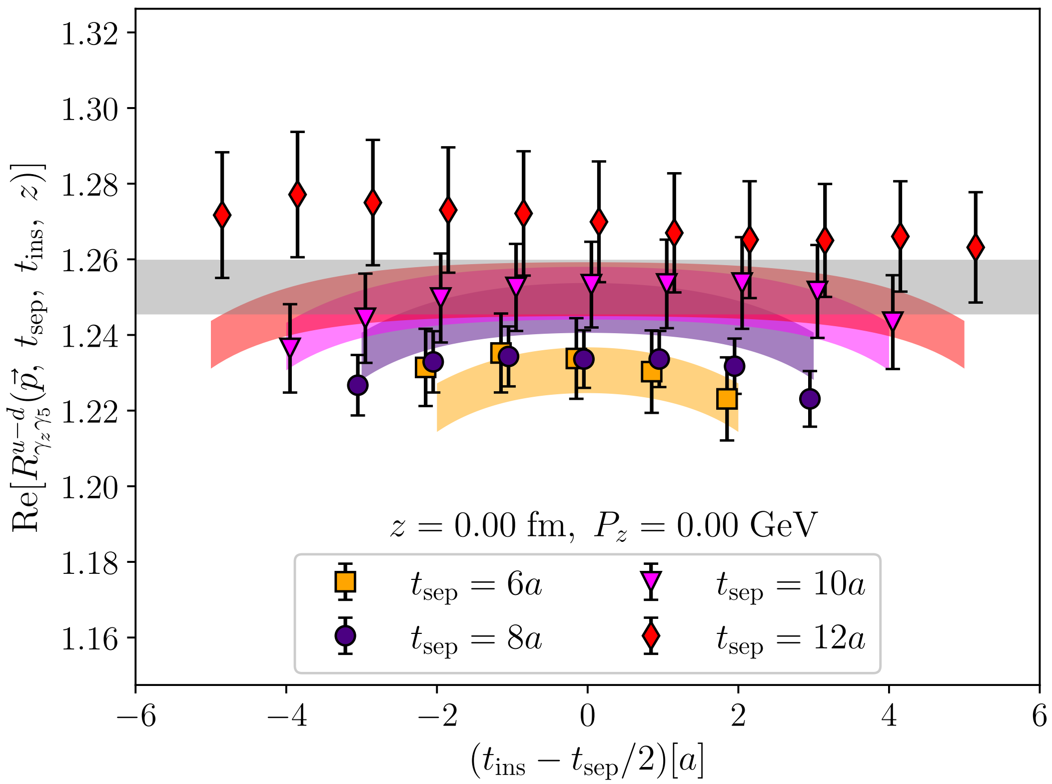

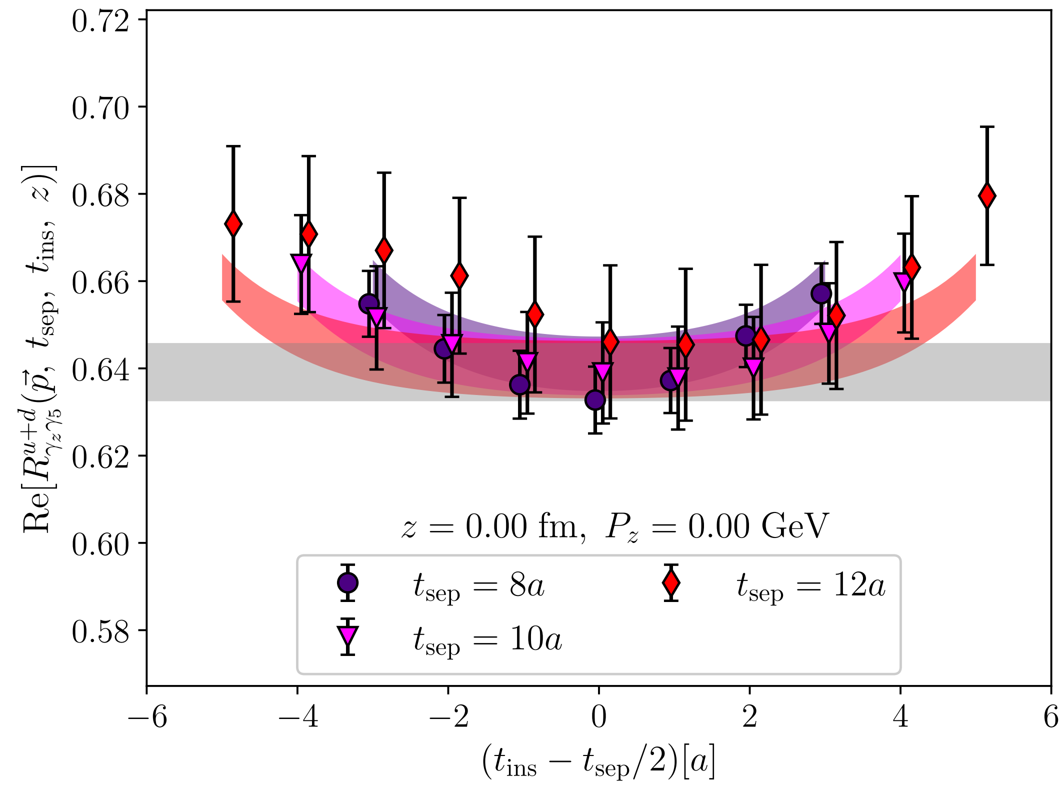

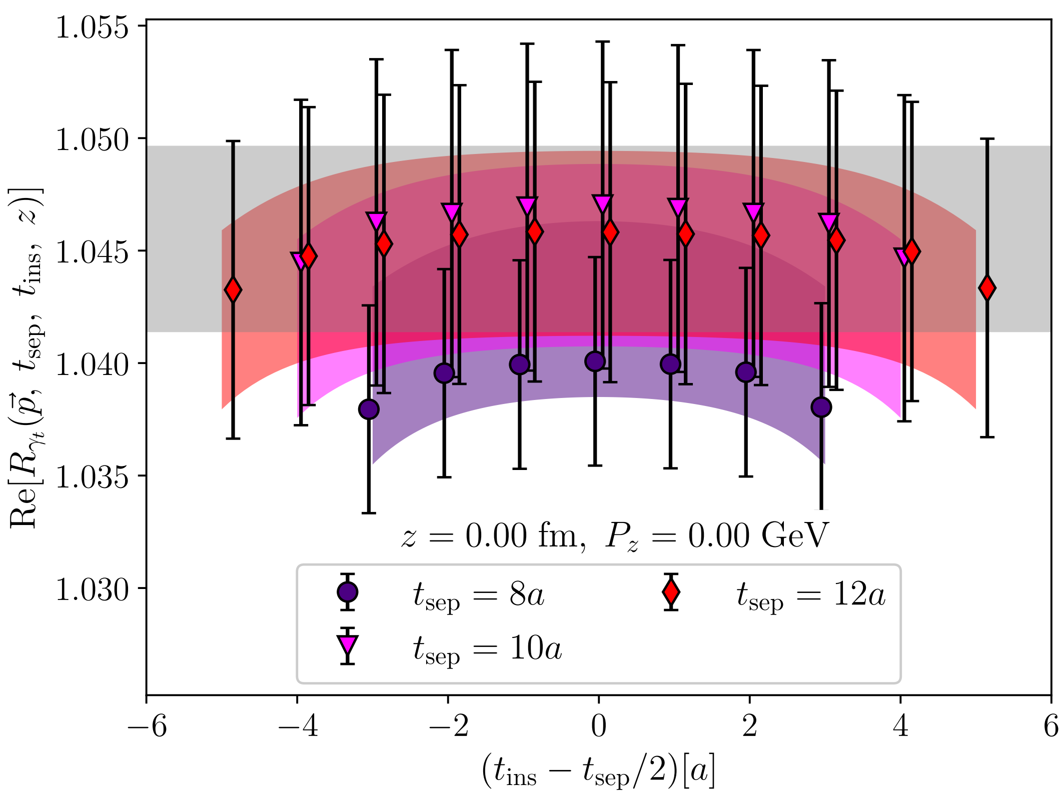

$$g_A^R = Z_A g_A^B = \frac{Z_A}{Z_V}\frac{g_A^B}{g_V^B}$$

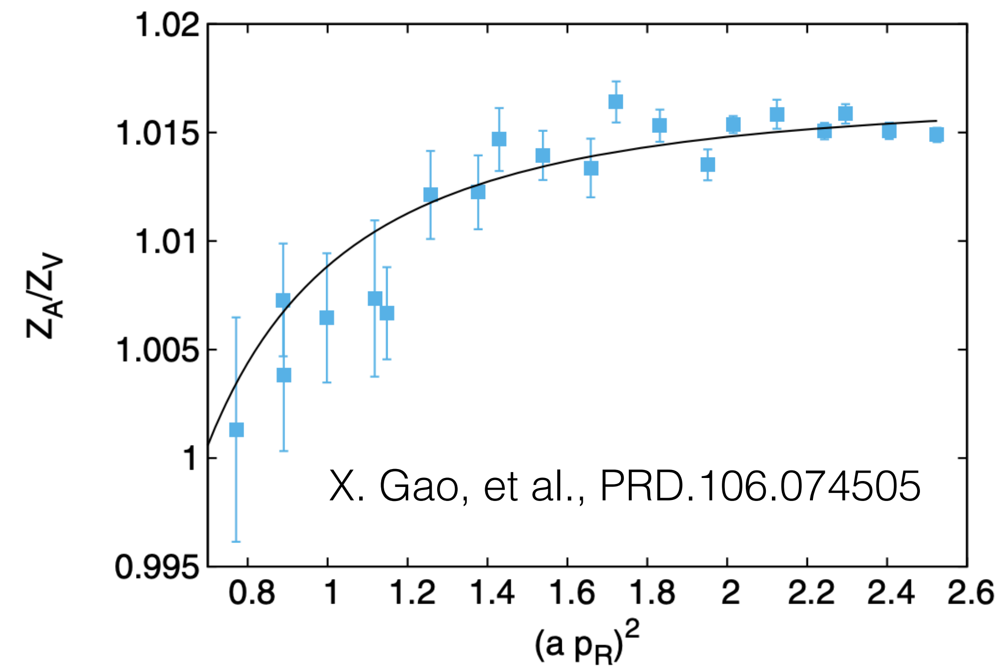

Backup: covariance matrix (I)

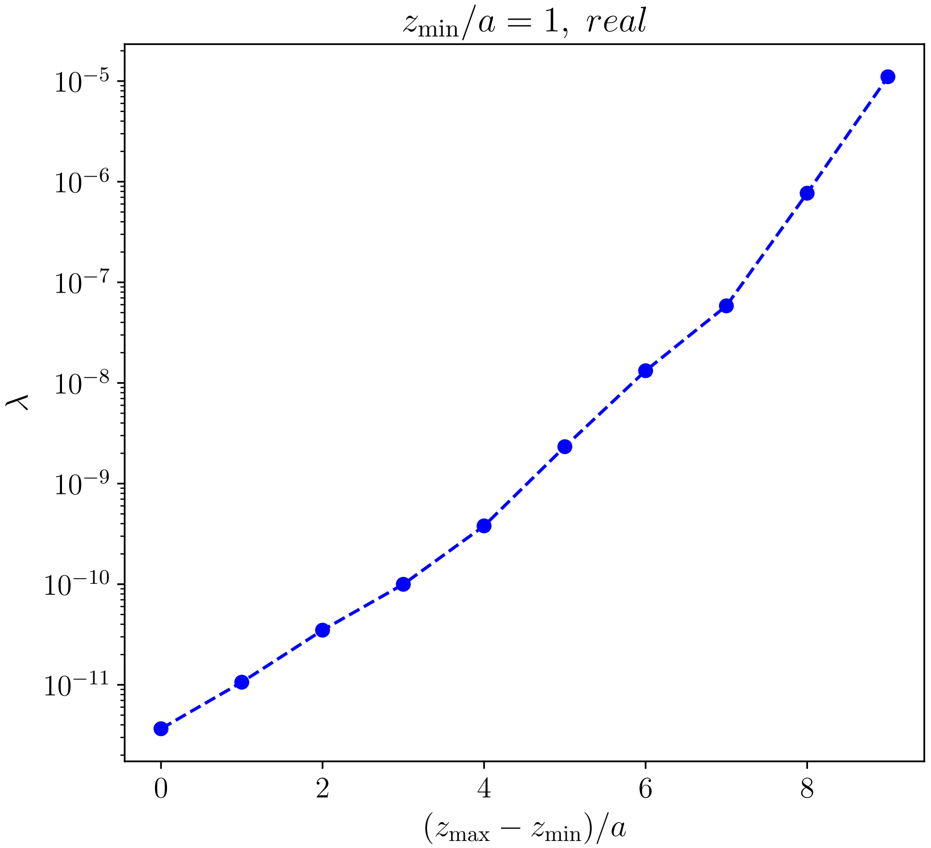

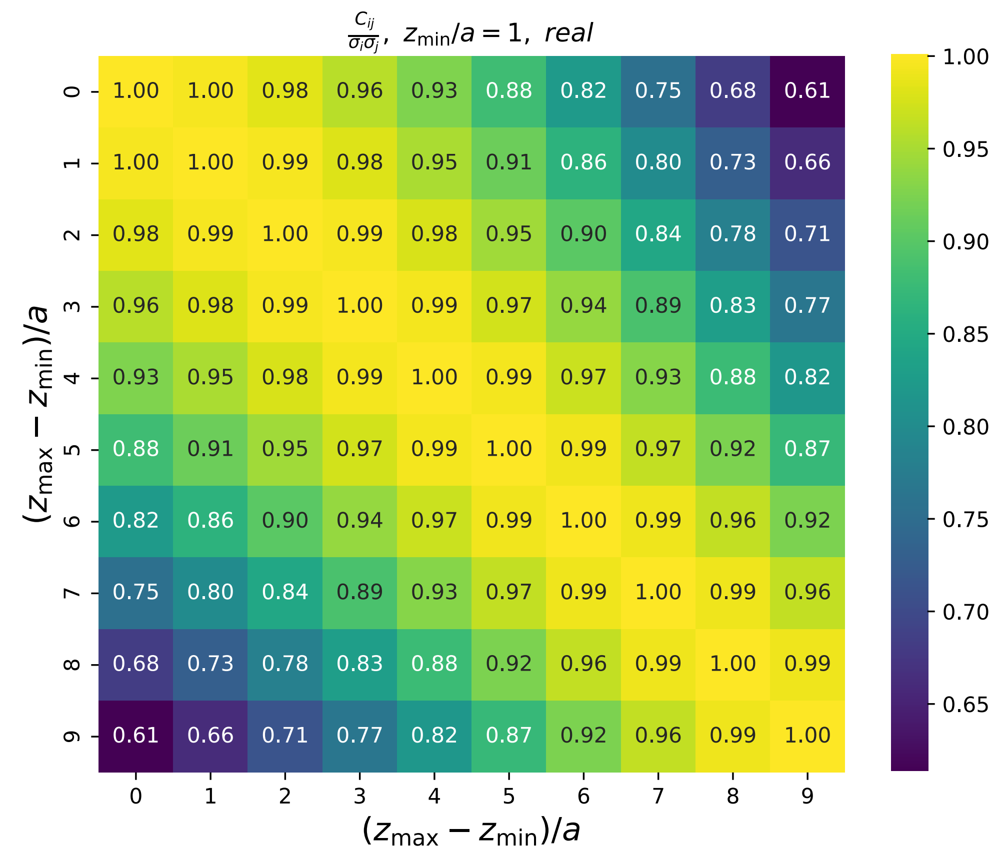

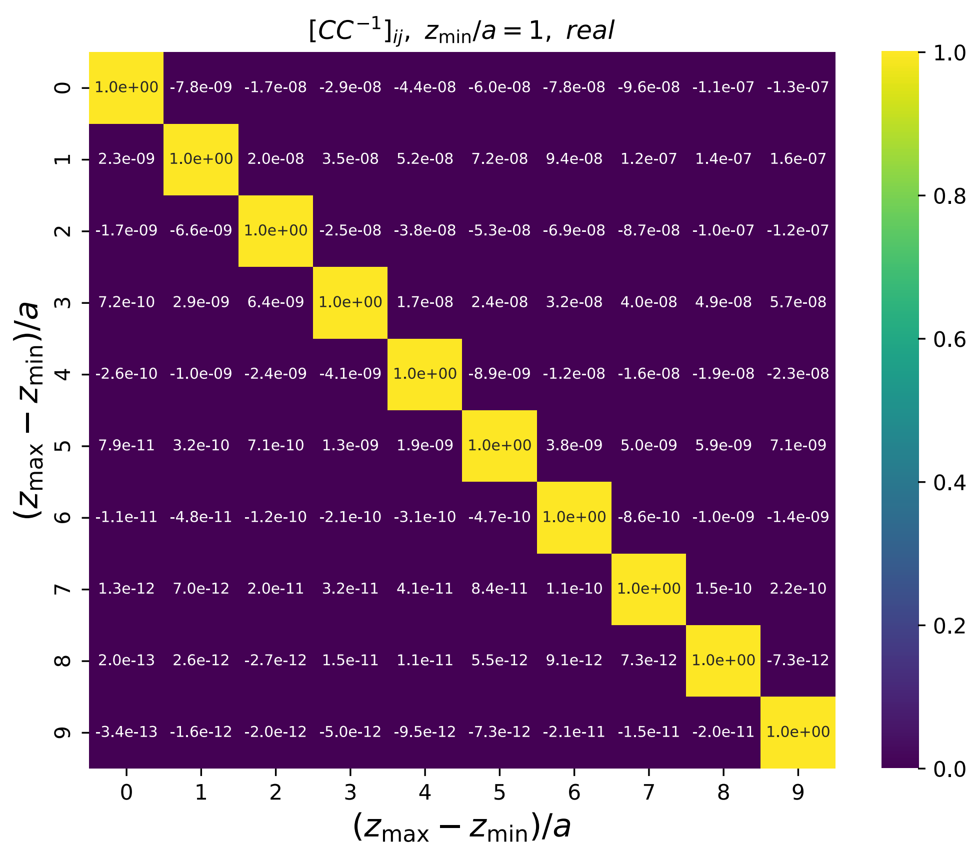

z_{min}=1a, z_{max}=10a

Strong correlation, particularly at shorter distances!

Backup: covariance matrix (II)

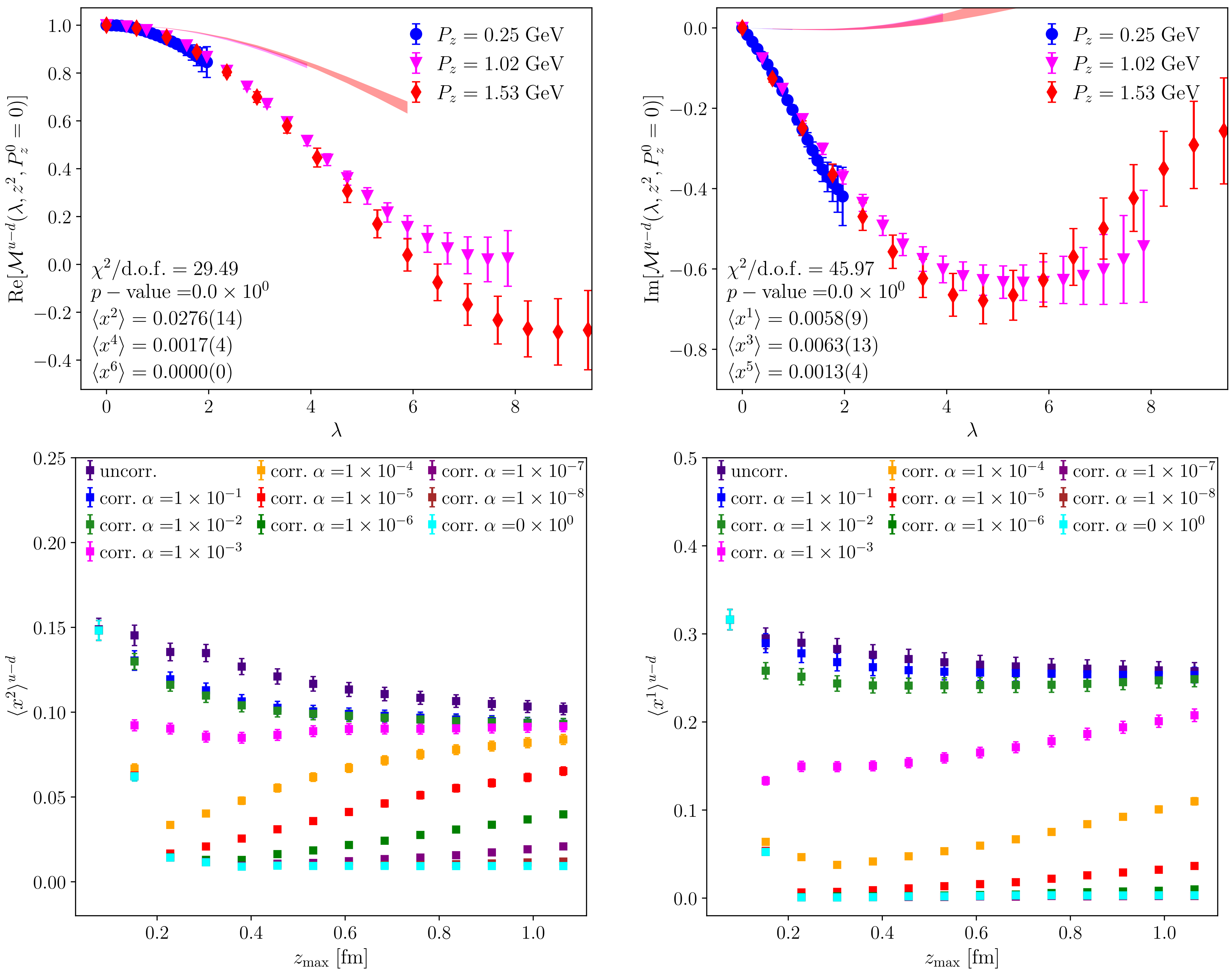

Backup: covariance matrix (III)

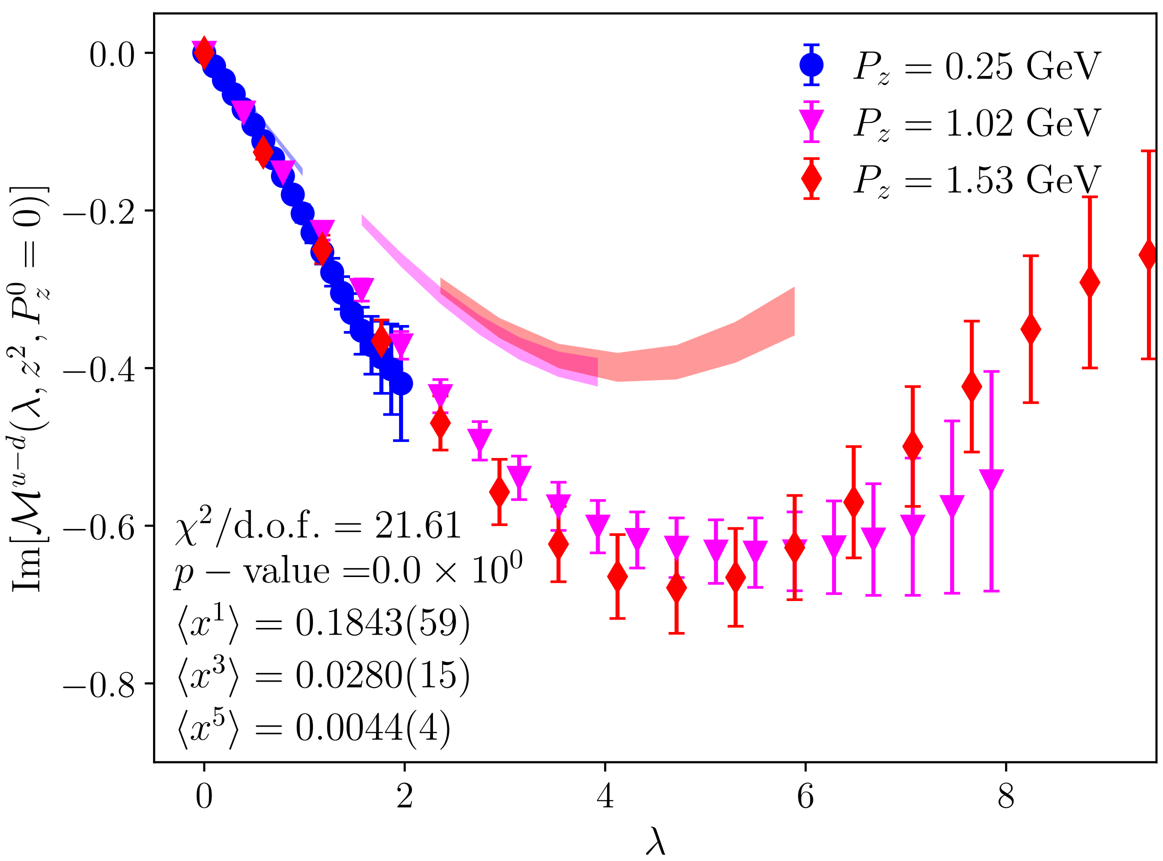

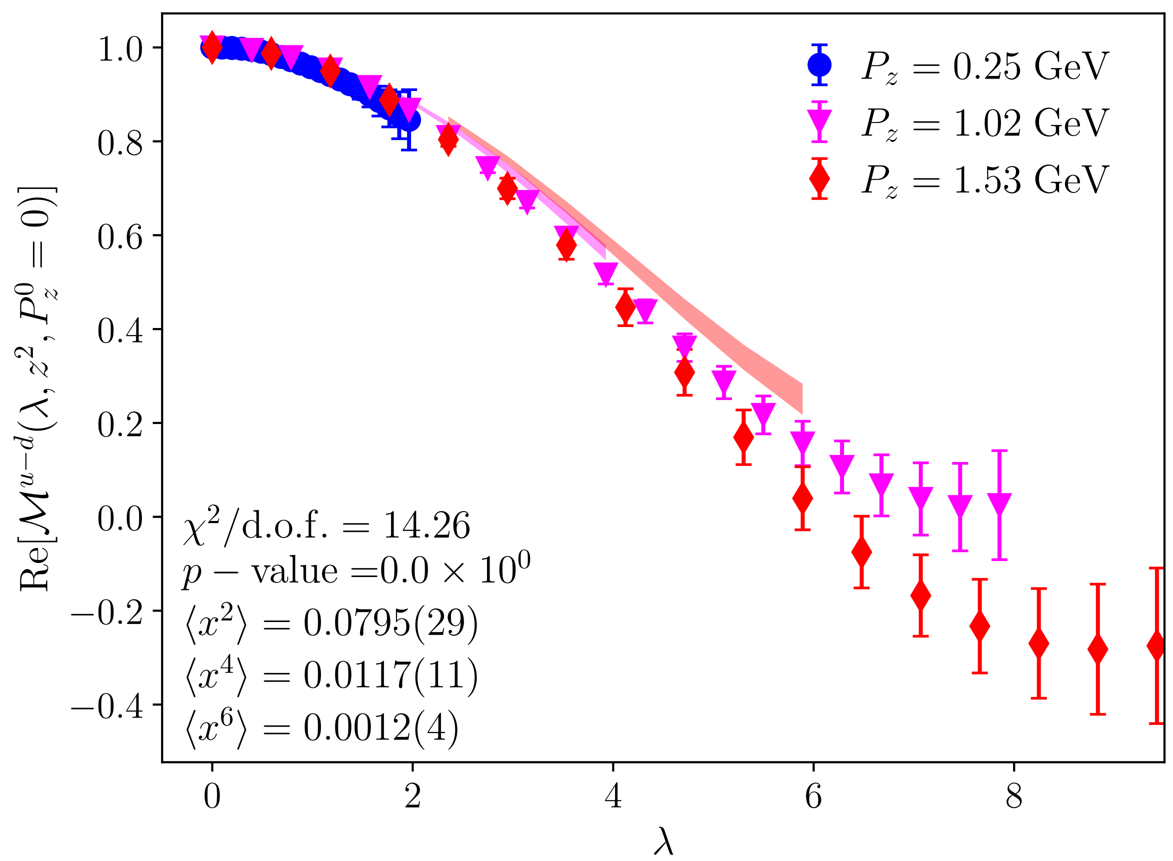

Backup: covariance matrix (IV)

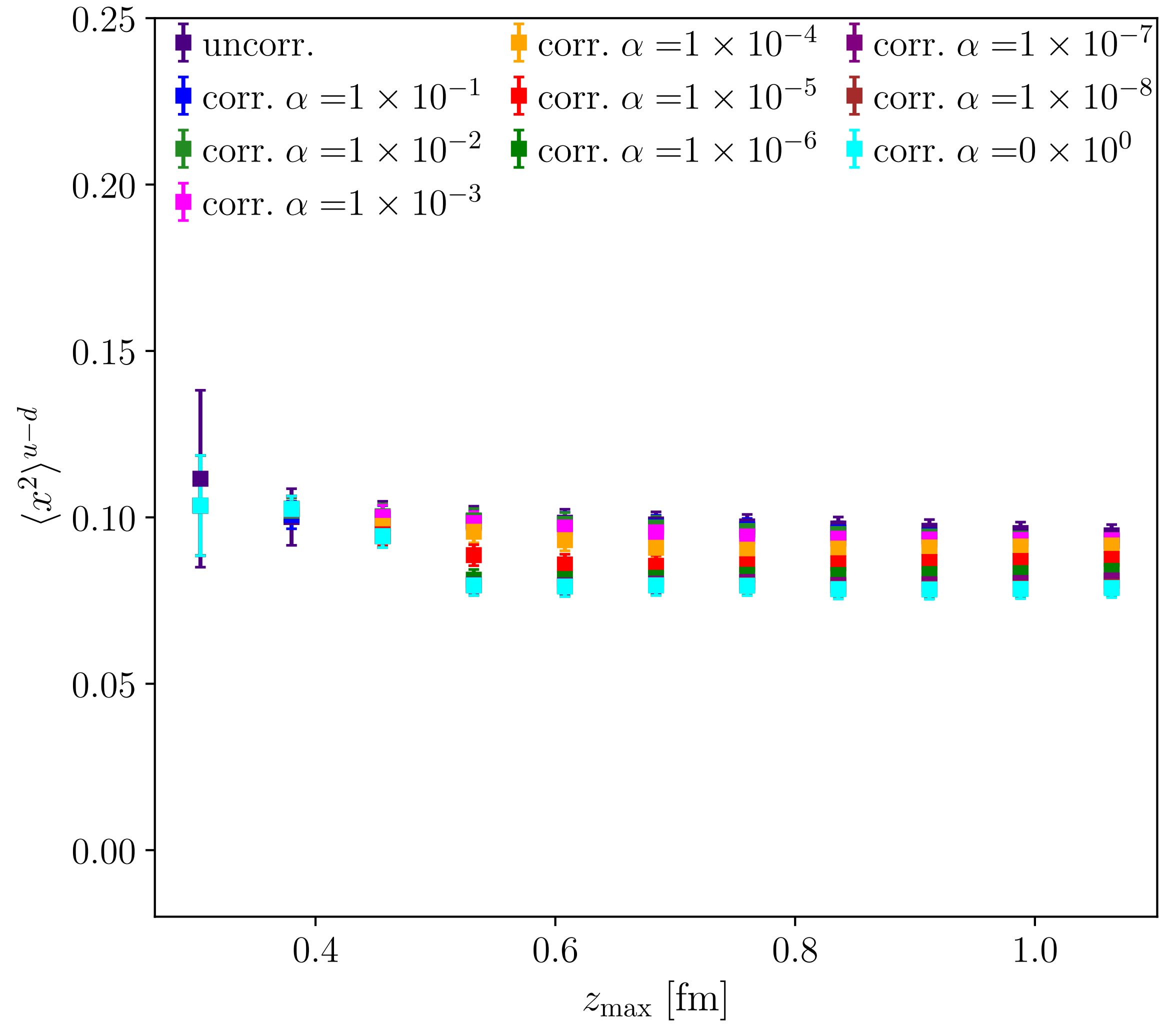

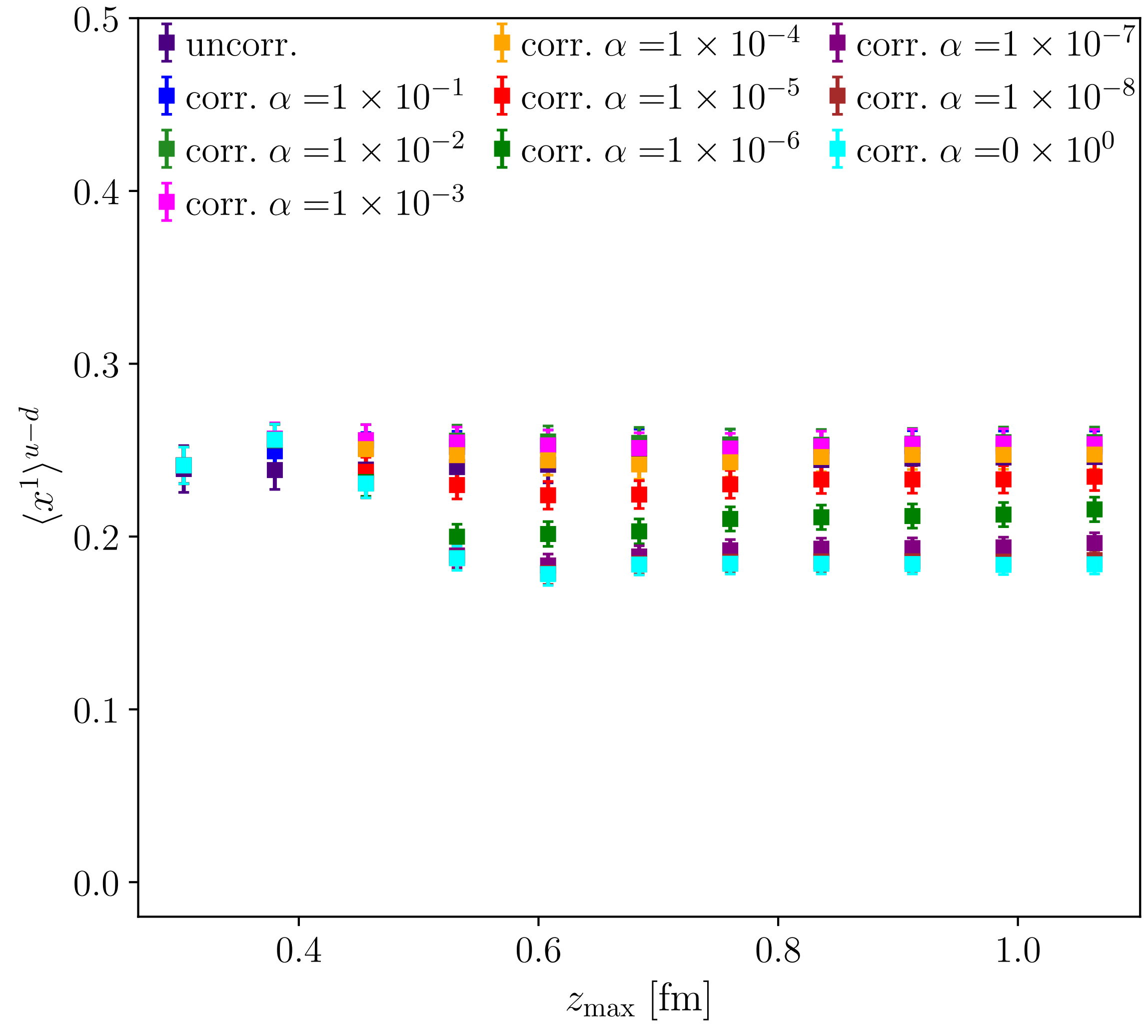

Backup: covariance matrix (V)

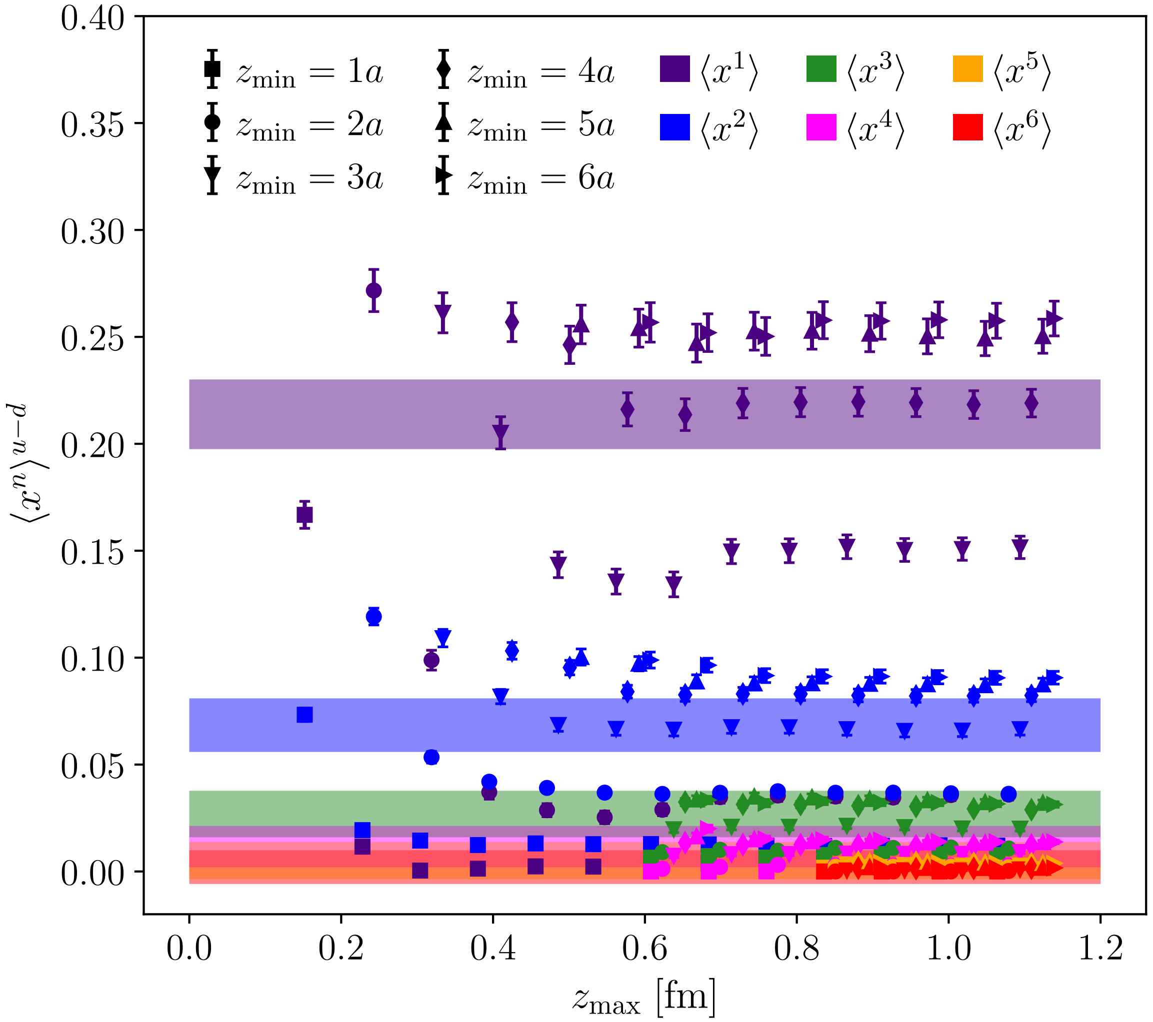

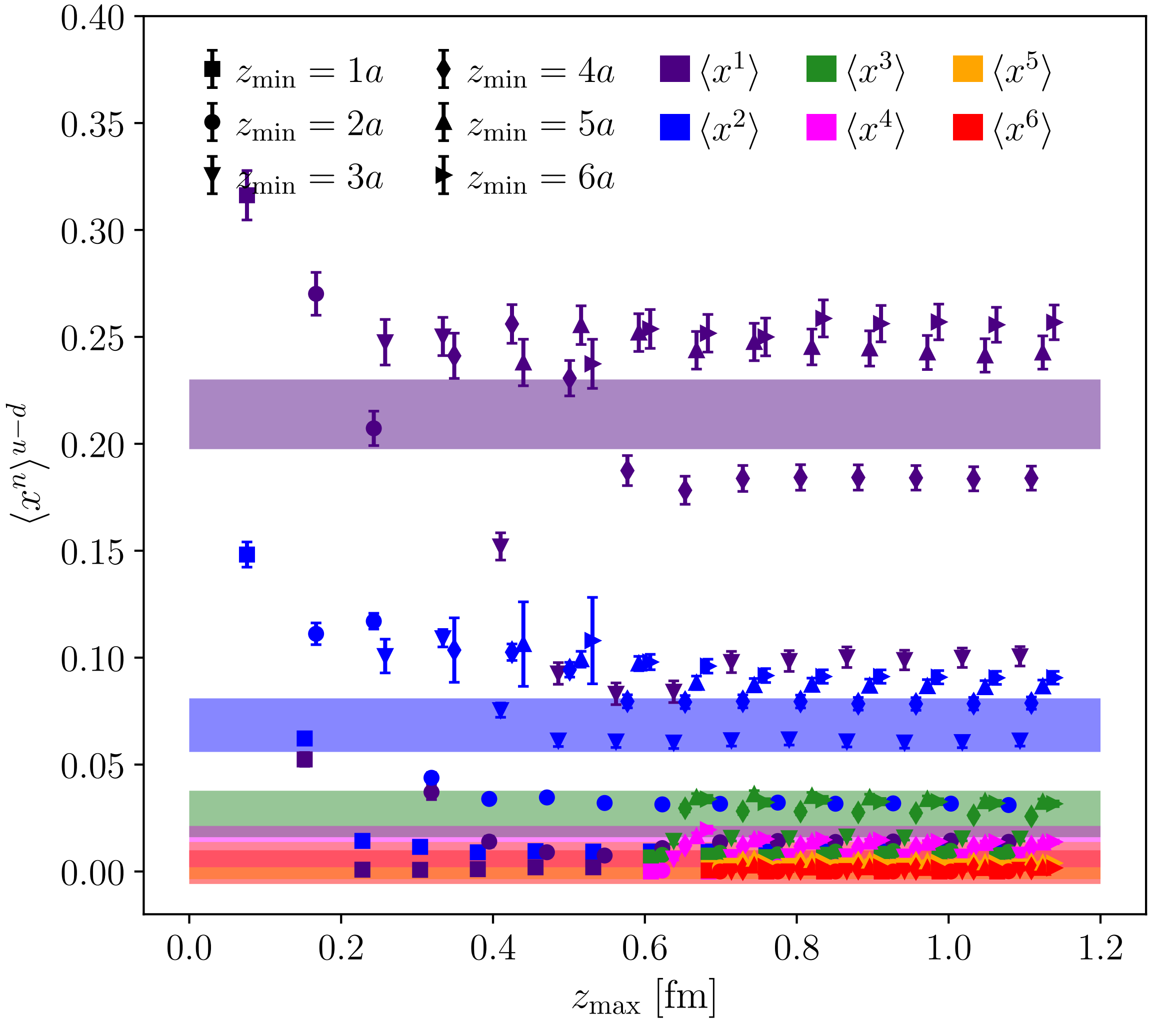

Backup: dependence on DNN parameters

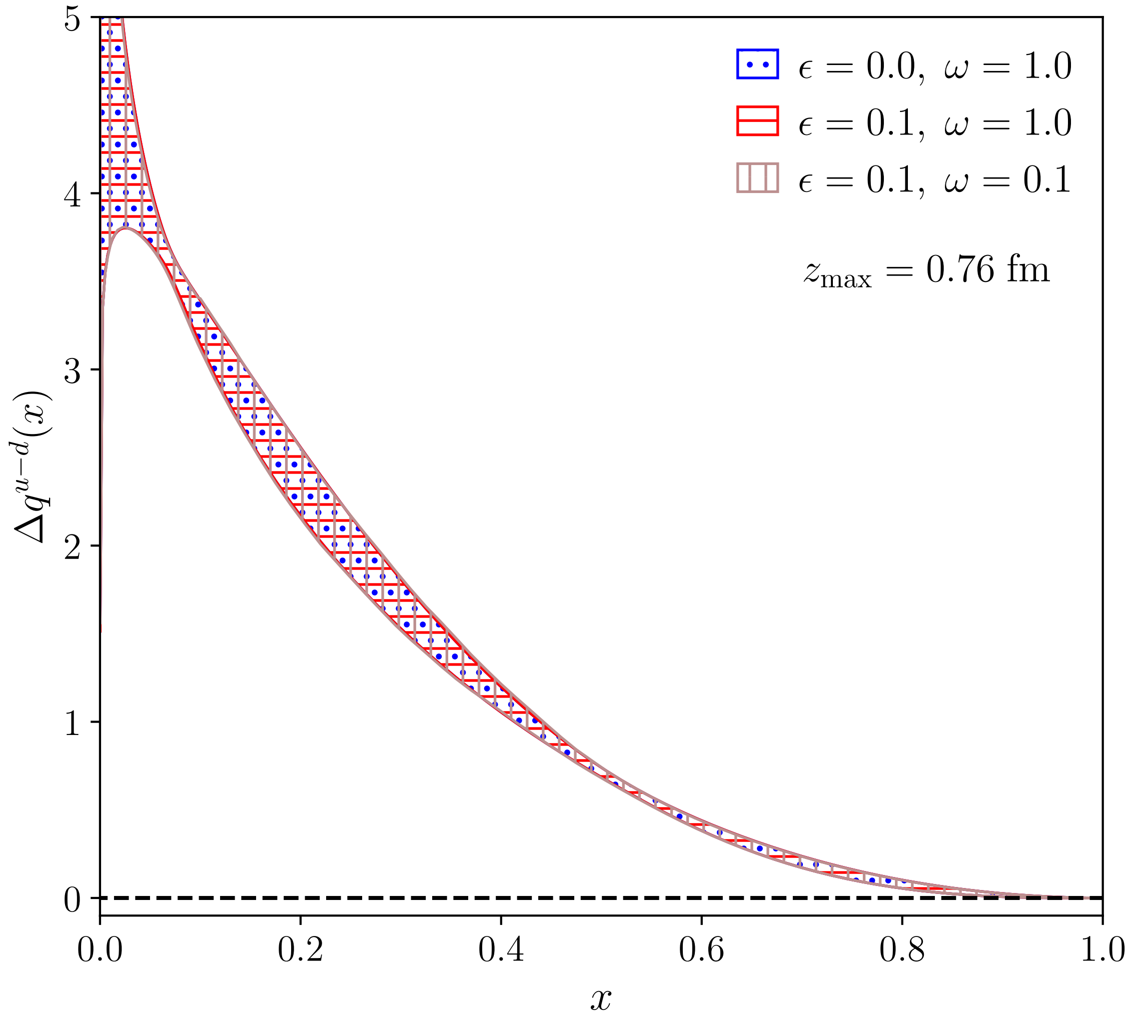

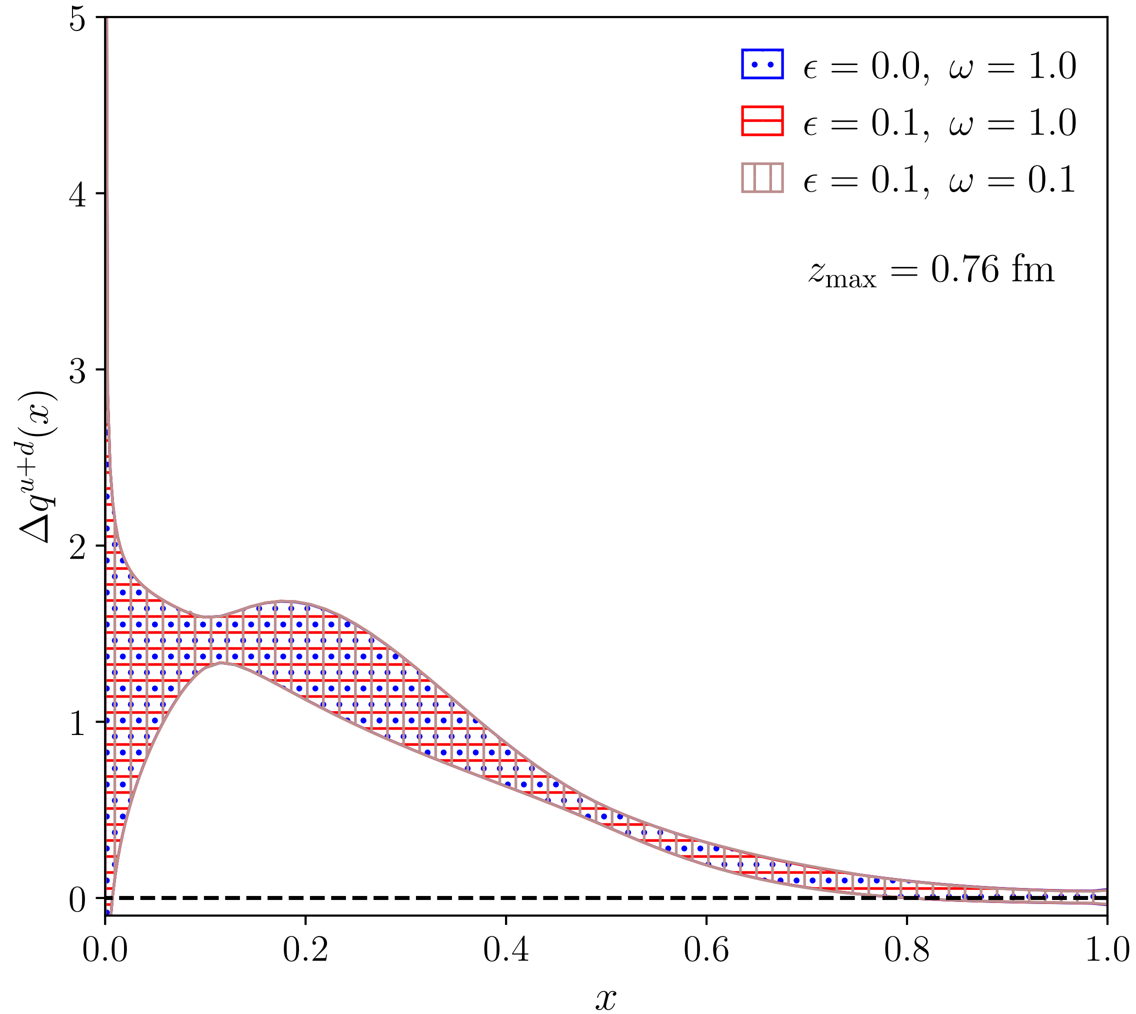

$$\text{Loss} = \frac{\eta}{2}\boldsymbol{\theta}\cdot\boldsymbol{\theta} + \omega||\nabla f_{\text{DNN}}|| + \frac{\chi^2}{2}$$

Backup: decaying model

$$\left[\frac{c_1}{(i\lambda)^a} + e^{-i\lambda}\frac{c_2}{(-i\lambda)^b}\right] e^{-\lambda/\lambda_0}$$

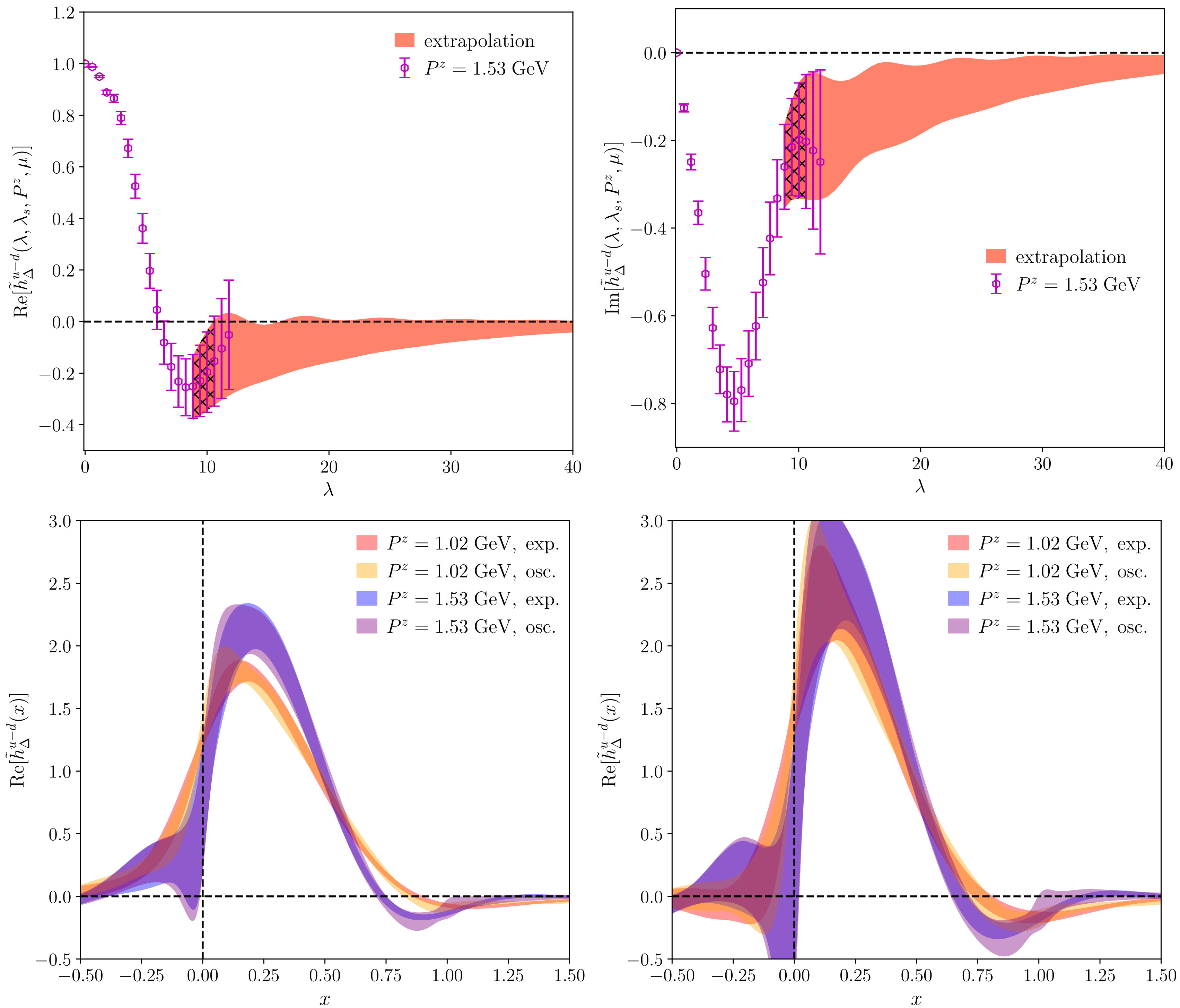

Backup: RI-MOM

Euclidean state with momentum squared $-p^2 \gg \Lambda^2_{\mathrm{QCD}}$ in a fixed gauge, and then defines $\overline{\mathrm{MS}}$ operators as,

$$O_{\overline{\mathrm{MS}}}(z,\mu) \equiv Z_{\overline{\mathrm{MS}}}(z,-p^2,\mu)\frac{O(z,a)}{Z(z,-p^2,a)}, \tag{13}$$

where $Z_{\overline{\mathrm{MS}}}$ converts the RI/MOM renormalized result to the $\overline{\mathrm{MS}}$ scheme. The gauge and $-p^2$ dependences cancel between two Z-factors. The r.h.s. has a proper continuum limit $a \to 0$ without divergences.

However, while the RI/MOM approach is justified for local operators, it has potential problems when applied to nonlocal ones. For instance, when z becomes large, $Z_{\overline{\mathrm{MS}}}(z,-p^2,\mu^2)$ contains IR logarithms of z and the perturbative calculation of z-dependence is not reliable. Moreover, although the RI/MOM factor $Z(z,-p^2,a)$ helps to cancel the lattice UV divergences, the composite operator at large-z contains non-perturbative physics as well. Therefore, both Z-factors contain non-cancelling non-perturbative effects which alter the IR properties of $O(z)$. Thus, the RI/MOM renormalization scheme is not reliable at large-z. Moreover, when gluon distributions are involved, it requires external off-shell gluon states which bring in potential mixing with gauge-variant operators and make things much more complicated [67].

arXiv:2008.03886